Year-round measurement of atmospheric volatile organic compounds using sequential sampling in Dronning Maud Land, East-Antarctica

Preben Van Overmeiren[a], Kristof Demeestere[a], Alexander Mangold[b], Andy Delcloo[b,c], Herman Van Langenhove[a], Christophe Walgraeve[a,*]

[a] Research group EnVOC (Environmental Organic Chemistry and Technology), Department of Green Chemistry and Technology, Faculty of Bioscience Engineering, Ghent University, Ghent, Belgium
[b] Royal Meteorological Institute of Belgium (RMI), Ukkel, Belgium
[c] Department of Physics and Astronomy, Ghent University, Ghent, Belgium

*Corresponding author: Christophe Walgraeve (Christophe.Walgraeve@UGent.be), Coupure Links 653, Ghent, Belgium

Highlights

- VOCs were measured year-round at the Princess Elisabeth Station in Antarctica.
- A home-made sequential sorbent tube autosampler was deployed to sample unsupervised.
- Two complimentary analytical techniques, TD-GC-MS and TD-PTR-Qi-TOFMS were used.
- First concentration data for atmospheric oxidation products in East-Antarctica.

Abstract

Antarctica is considered the most pristine environment on Earth but is also characterized by its unique conditions such as the strong polar vortex and extreme cold. A detailed understanding of volatile organic compounds (VOCs) and the atmospheric oxidation reactions they undergo is essential to document biogeochemical cycles and to better understand their impact on radiative forcing. This research aims to provide a unique dataset of oxygenated (O)VOCs occurring in the Antarctic troposphere and provide insights into their temporal behavior. A home-made sequential sorbent tube auto sampler was deployed at the atmospheric observatory of the Princess Elisabeth station (71.95° S, 23.35° E, 1390 m asl) to collect 20 samples during the period from December 2019 to October 2020. The samples were analyzed consecutively by TD-GC-MS followed by direct thermal desorption of samples in a high-resolution PTR-Qi-TOFMS.

Concentrations of 70 VOCs allocated to 4 different chemical groups (halogenated compounds, non-aromatic hydrocarbons, sulfur-containing compounds, and oxygenated aromatic and non-aromatic compounds) were determined. The results show temporal patterns for compounds such as bromoform (14 ± 6 ng/m^3) and OVOCs such as furaldehyde (24 ± 9 ng/m^3), amongst others, which are attributed to the seasonality of atmospheric conditions. Products of the atmospheric oxidation process show linear correlation indicating their mutual relationship and association with a common parent compound.

The usage of an autonomous autosampler in the extreme conditions of Antarctica was demonstrated and proved to be a powerful tool in the sampling of air in such a remote location. The novel approach of using two analytical techniques boasts increased sensitivity and a broad range of compounds that can be detected, yielding the first dataset of its kind for Antarctica.

Keywords: VOCs, OVOCs, Antarctic Atmosphere, Autosampler, TD-GC-MS, TD-PTR-Qi-TOFMS

1 Introduction

Despite their trace level concentrations, volatile organic compounds (VOCs) play an important role in the atmosphere and influence the global climate. Both anthropogenic activities, as well as biogenic processes, contribute to observed concentrations of VOCs in the troposphere. VOCs are important precursors of ozone and aerosols. Tropospheric ozone is a direct greenhouse gas and plays a key role in the oxidation of atmospheric VOCs, and it is a precursor of hydroxyl radicals in clean environments (Atkinson and Arey, 2003; Griffiths et al., 2021). Typical VOCs such as single-ring aromatic hydrocarbons have an atmospheric lifetime ranging from several hours to weeks, while there are notable exceptions on both sides of the range. Chlorofluorocarbons (CFCs) atmospheric lifetimes are in the order of decades while e.g. isoprene is transformed with an atmospheric lifetime of 1-2 hours in clean atmospheric conditions (Atkinson and Arey, 2003). Removal of VOCs from the atmosphere happens through the reaction with radical species (e.g. hydroxyl radicals, nitrate radicals, amongst others), photochemical reactions, and reactions with ozone finally resulting in a complete mineralization towards CO_2 and H_2O. Intermediate products formed during this process result in less volatile compounds with polar functionalities which might form so-called secondary organic aerosols (SOAs) after condensation. Typically, these can also be removed from the atmosphere by wet or dry deposition. Before their removal, SOAs have a substantial effect on the global climate by radiative forcing, both directly via aerosol-radiation interaction responsible for on average −0.22 (−0.47 to −0.04) $W.m^{-2}$ and indirectly as they act as cloud condensation nuclei (CCN), interacting with the cloud formation processes or changing the cloud microphysics, responsible for a radiative forcing of on average −0.84 (−1.45 to −0.25) $W.m^{-2}$ (Forster et al., 2021; Karset et al., 2018; Koppmann, 2007; Mellouki et al., 2015; Shrivastava et al., 2017). Next to the effect on Earth's energy budget, clouds play an important role in the hydrological cycle. In Antarctica specifically, precipitation is the only positive contributor to surface mass balance (Boucher et al., 2013; Gorodetskaya et al., 2015; Hu et al., 2013). The atmospheric conditions in the polar regions are very distinct as specific phenomena such as the polar day and night, powerful polar vortices, and strong UV radiation don't occur anywhere else in the world (Slusher et al., 2010).

To understand the influence of VOCs on atmospheric processes, concentration data are of paramount importance. However, in Antarctica, this data remains very scarce. Challenges such as the extreme cold, complicated logistics, and the necessity for robust sampling equipment are the root cause that such a limited number of studies on these volatile compounds in Antarctica exist. Since the first publication on this topic in 1989, only 22 scientific reports on measurements of VOCs in Antarctica have been published. The first reports describe the sampling and analysis of light nonmethane hydrocarbons (NMHC) (C_2-C_3) and chlorinated hydrocarbons (CHCs) between 1982 and 1989, using canisters for sampling at Neumayer I station and Scott Base (Rudolph et al., 1992a, 1989). (Clarkson and Martin, 1997) reported a longer time series with shorter intervals for ethane and propane using canister sampling at Scott Base from 1990 to 1996. They observed that mixing of air between mid and high latitudes south is possible and takes place in a timespan comparable to the lifetime of propane (two weeks).

CFCs are man-made chemicals and are amongst the longest-living species in the atmosphere. They are monitored all over the world, including Antarctica, because of their relevance in the destruction of stratospheric ozone and their global warming potential. In the lower atmosphere, however, their high inertness makes they don't participate in tropospheric chemistry (Koppmann, 2007). (Bruner et al., 1994) used on-site sampling and online GC-ECD and on-site sampling, with off-site analysis to determine CFCs in the region around Terra Nova Bay during the summer of 1990/91. Online-GC is implemented for near-continuous monitoring of VOCs, but it requires regular maintenance and ultra-pure gases and supplies on location, although with the advance of thermo-electric cooling the need for liquid nitrogen for the cryogenic trap is eliminated. For off-site analysis, these logistics are far less complicated and it can be implemented by sampling the air using canisters or sorbent enrichment (Bruner et al., 1994). In the latter case, active sampling by pumping one or two liters of air over a sorbent trap consisting of graphitized carbon black (between 400 and 800 mg depending on the type) was used, after which the sample was analyzed in Italy via GC-HRMS. During the summer of 1993/94, (Bruner et al., 1996) sampled C_1-C_2 halogenated hydrocarbons in the same region using air canisters and off-site analysis with GC-ECD. They stated that the canister sampling procedure is much easier compared to sorbent enrichment when sampling in Antarctic conditions. Canister sampling remained the preferred method for sampling CFCs and was used at Palmer and South Pole station by (Rasmussen and Khalil, 1999) and in the Ross Sea region (Zoccolillo et al., 2010, 2009).

(Beyersdorf et al., 2010) quantified methane, six C_2-C_4 hydrocarbons, benzene, five alkylnitrates, and compounds associated with marine biogenic emissions such as bromoform, methyl iodide, and dimethylsulfide (DMS) during the ISCAT and ANTCI program (from November 2000 to October 2001, and from November 2003 to November 2006). Samples were collected year-round using canisters at the South Pole Station and analyzed by GC-FID, GC-ECD, and GC-MS. Benzene, typically associated with anthropogenic sources, is only reported in Antarctica in one other instance with (Read et al., 2007) reporting on seasonal trends of C_2-C_5 hydrocarbons and benzene using an online-GC-FID at Halley V station. Both studies concluded that benzene concentrations are a factor of 4 to 10 higher in winter (17 and 18 ppt_v) compared to summer (4 and 2 ppt_v).

DMS is the dominant source of organic sulfur in the atmosphere and is readily oxidized to methane sulphonic acid (MSA), dimethylsulfoxide (DMSO), and non-sea salt sulfate particles ($nss\text{-}SO_4^{2-}$) contributing to marine aerosols and forming CCN. High variability in DMS concentrations is found between coastal and inland stations, as well as a strong seasonality. In general, much lower concentrations of DMS and oxidation products are observed at stations away from the coast. (Beyersdorf et al., 2010; Swanson et al., 2004) and (Preunkert et al., 2008) reported DMS mixing ratios, ranging from below the detection limit of 1-2 ppt_v (for most of spring and summer samples) to 7.3 to 11 ppt_v during winter, at the South Pole and Concordia station. Concentrations at coastal stations are higher, as reported by (Read et al., 2008) at Halley station (2004-2005) and by (Preunkert et al., 2007) at Dumont D'Urville station (1998-2003). Reporting average concentrations range between 24 and 86 ppt_v during summer and up to a maximum of 418 ppt_v. This is in accordance with (Koga et al., 2014) who reported concentrations between 50 and 700 ppt_v during ship-based measurements using a proton transfer reaction mass spectrometry (PTR-MS) in the Southern ocean, during the austral summer of 2009-2010. PTR-MS allows measuring trace gases in an online manner by directly introducing the ambient air in the instrument followed by a soft ionization of the VOCs by H_3O^+, eliminating the need for a sample trap and carrier gas (Pleil et al., 2019; B. Yuan et al., 2017). Since advances in PTR-MS which led to increased sensitivity are only recent, few measurements in remote environments are reported. To our knowledge (Koga et al., 2014) are the only researchers who published about the usage of PTR-MS in Antarctica.

Oxygenated VOCs (OVOCs) originating from photochemical oxidation reactions are likely to be present in the Antarctic troposphere as all precursors are present. Only (Ciccioli et al., 1996a) published data dedicated to OVOCs in Antarctica which were sampled using canisters. A total of 76 different VOCs were identified at 6 sample sites located near Terra Nova Bay during the summer of 1993, proving the ubiquitous occurrence of these compounds.

Although a limited amount of data on VOCs in Antarctica are available, much less is known about their seasonality. To better understand the seasonality of these compounds and gain insight into the atmospheric processes in remote environments, year-round measurements, consisting of several consecutive discrete samples to construct a time series, are required. While online-GC has major advantages, sampling combined with off-site analysis is better suited to run unattended for long time periods. Automated sequential whole-air sampling can be performed using a rack of multiple canisters with an electronically controlled valve (Atlas and UCAR/NCAR - Earth Observing Laboratory, 2009; Lerner et al., 2017). Alternatively, sorbent enrichment-equipped sequential samplers can be used, which are much more compact and combine the sampling and sample enrichment in one step.

As neither of the sequential sampling techniques has been used in Antarctica, and no commercially available systems are intended for such extreme environments, we developed a novel automatic tube sampler. We conducted a sampling campaign at the Belgian research base Princess Elisabeth in Dronning Maud Land from December 2019 to October 2020, to increase the knowledge of the concentrations and seasonality of (O)VOCs in the lower atmosphere in East-Antarctica. Two instrumental analytical methods were developed in order to analyze the sampled sorbent tubes. The first encompasses thermal desorption (TD) followed by traditional GC-MS analysis, whereas the second method is based on a novel direct desorption of the sorbent tube into a high-resolution PTR-MS instrument. This research provides, for the first time, a dataset of (O)VOCs in East-Antarctica, providing 8 months of concentration data on 66 compounds.

2 Experimental

2.1 Chemicals and standards

Thirty-six VOCs with a purity of >99% were purchased at Acros Organics, BE or Sigma Aldrich, BE to make stock solutions for calibration of the TD-GC-MS and the TD-PTR-Qi-TOFMS instruments. Neat standards were thereby taken by volume (for liquids) or by weight (for solids) using a Sartorius analytical balance (0.1 mg resolution) and dissolved in methanol (Optima LC-MS grade, 99.8+%, Fisher Scientific, BE), leading to concentrations between 27.5 and 144.5 ng.µL^{-1}. To assure the stability of the solutions, the compounds were split over 5 individual stock solutions. The details can be found in S.I. 1. Perdeuterated toluene (toluene-d8, $C_7{}^2H_8$) (99.5+ atom%D; Acros Organics, BE) was used as an internal standard (IS). Helium and nitrogen gas were used during sample preparation and analysis, and were of Alphagaz2 quality, 99,9999+% pure ($C_nH_m \leq 0.1$ ppm$_v$ and $H_2O \leq 0,5$ ppm$_v$) (Air Liquide, BE).

2.2 Sampling location

The Princess Elisabeth Antarctic station (PEA) is a zero-emission research base, located close to the Sør Rondane mountains in Queen Maud Land, East-Antarctica at 70° 57’ S, 23° 20’ E and 1390 m.a.s.l. It is inhabited during the Antarctic summer between November and February and is operated via remote access during the rest of the year. It is close to the Antarctic plateau (50 km) and the Ragnhild coast (200 km) and is located in a relatively mild microclimate. The site is dominated by an easterly wind year-round (> 90%) and air temperatures vary between -36 and -5 °C (Gorodetskaya et al., 2013; Pattyn et al., 2009). Air was sampled using a newly developed autosampler (Section 2.3) on the roof of the atmospheric measurement shelter where, since the base was inaugurated in February 2009, several atmospheric aerosol monitoring instruments such as an aethalometer, a nephelometer, an optical particle sizer, and a condensation particle counter have been running near continuously (Herenz et al., 2019). In addition, on the roof of the PEA station, a ceilometer and a micro-rain radar have been installed for monitoring cloud and precipitation characteristics (Gorodetskaya et al., 2015).

2.3 Automated active sampling

A new automated sequential sampler (ATS-50) was developed and optimized in-house within the EnVOC research group of Ghent University, Belgium, to sample VOCs autonomously over a period of one year via active sampling on stainless steel sampling enrichment tubes filled with 200 mg Tenax TA as a sorbent. The developed sampler uses a rotating manifold and stepper motor to select the sampling positions (Figure 1) and was controlled using an open-source Arduino microcontroller. Passive uptake of VOCs by diffusion whilst the tubes are inserted into the autosampler is minimized by the use of sorbent tubes outfitted with a diffusion limiting insert (SafeLok) increasing the diffusion path length (Markes international, 2014; Woolfenden, 2012; Woolfenden and Cole, 2003). The autosampler is designed to be equipped with up to 50 sorbent tubes and 5 blanks which are held in an identical configuration, but not sampled. During the sampling campaign discussed in this paper, 25 samples and 3 blank positions were used. The main body of the sampler consists of food-safe polyacetal polymer (POM) and stainless steel. All tubing and connections used are made of either PTFE or stainless steel. Developing our own autosampler was essential to achieve the necessary flexibility in the programming of our sampling campaign, and to sample under extreme conditions posed by the high wind speeds and cold temperatures. Mechanical and electrical components which remain stable at low temperatures were selected for its construction. An accurate sample volume is crucial for the final calculation of the VOCs concentration. Therefore, a Honeywell Zephyr HAF amplified flowmeter (0-200 sccm) was inserted between the sample tubes and the pump (Thomas G12/02EB, oil-less rotary vane, Germany). Flowrate and sampling time were logged continuously on an industrial (-40°C) SD card (Innodisk 512 MB). To validate the flowrate, a Safelok equipped sorbent tube was installed in the sample path and the pump was run with a PWM (pulse-width modulation) duty cycle of 4.69%. A calibrated TSI 4140 flowmeter was then connected to the sample tube inlet, and the instrument was run for 3600 minutes. An average flow of 36 sccm with a relative standard deviation (RSD) of 7% was measured on the internal flowmeter, while the calibrated flowmeter measured values between 35 and 38 sccm (S.I. 2), confirming that the internal flow meter can be used to determine the sample volume. The autosampler was programmed at a flow rate of 30 sccm for 3 days resulting in a total planned sample volume of 130 L on 1 sorbent tube. After the set sampling period, the sampler was programmed to enter standby mode for 10 days, after which the next cycle was initiated.

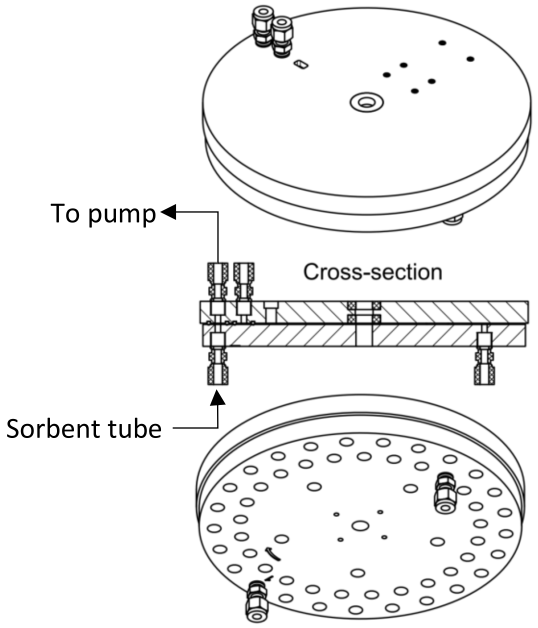

Figure 1: Drawing of the upper and lower assembly of the autosampler. The two plates (POM) rotate against each other, and an air-tight connection of the sampling line is established with O-rings. Alternating the two rows of sample positions accommodates for 50 samples on a limited surface. Only 2 of the 50 sample tube connectors are shown for the sake of a clearer drawing.

2.4 Sample preparation

All sorbent tubes were conditioned in a modified GC oven using helium fed through a stainless-steel manifold. Care is taken that the helium is flowing in the desorption direction of the tube at a flow rate of at least 100 mL/min. The tubes are kept at 300 °C for 1 hour, followed by another hour at 320 °C. After conditioning, tubes are capped using ¼” brass end caps (B-400-C, Swagelok, USA) fitted with one-piece ¼” PTFE ferrules (BGB Analytik Benelux, NL). To correct for the variability of the mass spectrometer’s response, the tubes are loaded with an internal standard. From a 2-phase (air/water) system, 10.8 ng gas-phase toluene-d8 was added to each tube using a gastight syringe and flushed with 300 mL helium using a 100 mL/min flow through a heated (150 °C) injector as described in (Demeestere et al., 2008). The sample tubes were transported to Antarctica in 500 mL amber glass bottles with a PTFE liner in the cap (Wheaton). To guarantee a good seal, the thread of the bottle was wrapped with PTFE tape and marked to ensure that the bottles were not opened during transport. Sampling tubes were mounted into the autosampler at the sampling position in Antarctica, and after 1-year sampling, the samples were collected during the subsequent polar expedition, stored in the amber glass bottles, and reshipped to Belgium in cold chain cargo (-20 °C) where they were stored in a freezer (-21°C) until analysis.

2.5 Instrumental analysis

The collected samples were analyzed following two discrete approaches. Firstly, the samples were analyzed by TD-GC-MS. The split flow, containing 75% of the original sample material, was recollected on a conditioned sorbent tube (200 mg Tenax TA). The recollection tube was then analyzed by an innovative and in-house developed TD-PTR-Qi-TOFMS combination which couples a thermal desorber to a high-resolution PTR-MS. A graphic representation of this sequence is given in S.I. 3.

2.5.1 TD-GC-MS analysis

Samples were analyzed on a 2-stage thermal desorption GC-MS system. Thermal desorption was performed at 260°C using a helium flow of 20 mL/min for 10 min using a Markes (Llantrisant, UK) series 2 Unity coupled with an Ultra autosampler. The analytes were refocused on a microtrap containing 29 mg Tenax TA 35/60 and 28.3 mg Carbograph 1TD 40/60 held at -10°C. The thermal desorption parameters are given in Table 1. The GC injection step embodies rapidly heating the microtrap to 280 °C and is held for 3 minutes. A helium stream carries the analytes via a deactivated fused silica transfer line (180 °C) to a FactorFour VF-1ms GC Column (Varian, Belgium; 100% dimethylpolysiloxane, 30m x 0.25 mm x 1 µm). Column head pressure was set at 50 kPa resulting in a 1.75 mL/min column flow. A 5 mL/min split was used during the trap desorption with the split flow recollected on a conditioned Tenax TA sorbent tube. The GC (Focus GC, Thermo Scientific, US) oven temperature was initially kept at 35°C (for 10 minutes) and then ramped in four stages, i.e. 35°C to 60°C at a heating rate of 2°C/min, 60 to 170°C at 8°C/min, 170 to 220°C at 15°C/min, and finally, at a heating rate of 15°C/min, a temperature of 240°C was reached and held for 10 min. After separation, the analytes were ionized by electron ionization (70 eV) and analyzed by a DSQ II mass spectrometer (Interscience, Louvain-La-Neuve, BE). The MS-transfer line was heated to 240°C. Chromatographic and MS data were recorded and processed using Xcalibur (version 2.2, Thermo Scientific).

2.5.2 TD-PTR-QiTOFMS analysis

A high-resolution PTR-Qi-TOFMS instrument (Ionicon, Austria) was hyphenated to a thermal desorption system consisting of a Unity and an UltraTD (Markes, Llantrisant, UK). This home-made setup allows for direct desorption of the sorbent tube containing the recollected sample (see section 2.5.1) into the PTR-Qi-TOFMS. The analytes are ionized by chemical ionization (using H_3O^+) and subsequently analyzed by high-resolution time-of-flight mass spectrometry. The used TD settings are listed in Table 1. Nitrogen (Alfagaz 2, Air Liquide) was used as a carrier gas for the thermal desorber. Oxygen and low molecular weight VOCs were scrubbed from the nitrogen with a 130cc Zpure (BGB) polygas I stainless steel inline gas purifier. The analytes were carried from the Unity to the interface via a Hydroguard fused silica capillary (Restek, 0.25 mm ID, 130 cm length) transfer line heated to 120 °C. The interfacing between the two instruments is schematically depicted in Figure 2. A stainless-steel tee union (1/16”, Swagelok) was used to dilute the gas flow (8 sccm) coming from the thermal desorption unit with nitrogen (diluent gas) to compensate for the higher inlet flow (80 - 180 sccm) of the PTR-Qi-TOFMS instrument. The Unity transfer line was inserted 20 mm inside of the PEEK tubing which was connected to the PTR-Qi-TOFMS inlet. This avoids contact of the analytes with the metal surface. As the inside diameter of the PEEK (polyether ether ketone) tubing (1 mm) is larger than the outside diameter of the transfer line (0.37 ± 0.04 mm), it leaves enough space for nitrogen to be added in a way so disturbance of the flow is minimal. To avoid condensation of analytes on tubing or couplings, the hardware is encompassed in a thermostat oven kept at 100°C. Dilution happens at atmospheric pressure by drawing the nitrogen from a glass gas bulb through which a 600 mL/min N_2 flow from a generator is kept. A Honeywell HAF flowmeter was used to monitor the flow to the interface. The diluent gas was pre-heated using a 1 m coil of 1/16” stainless steel tubing inside the heated chamber. A 1/16” PEEK straight union (Valco) was used to connect the PEEK tubing carrying the diluted stream to the inlet tube of the PTR-Qi-TOFMS (1 mm ID PEEK tubing) which was heated to 120°C.

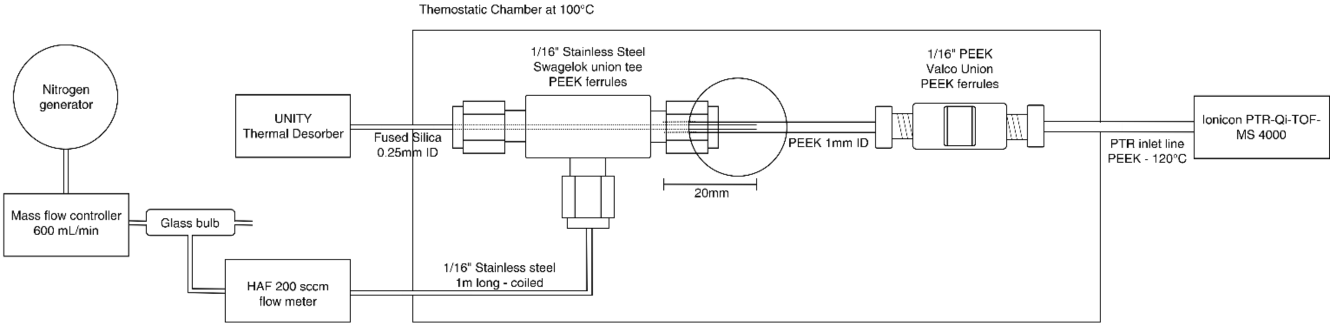

Figure 2: Diagram showing the interfacing between the Unity thermal desorber and the PTR-MS inlet.

It is important to set the dilution appropriately to avoid overloading the detector. Dilution factors can be adjusted by changing the inlet flow with a flow controller on the inlet line of the PTR-Qi-TOFMS. The flow through the Unity (Q_{unity}) during desorption is solely controlled by the carrier gas pressure which is regulated at 0.5 bar resulting in a flow of 8 sccm during trap desorption. Thus, by setting the inlet flow of the PTR-Qi-TOFMS, the flow of the diluent gas ($Q_{diluent}$) is established as it will compensate for the difference in flows. During the analysis of the samples, the inlet flow was always set to 165 sccm. Changing the post tube desorption split flow (Q_{split}) (0-40 mL/min range) also adds an additional sample dilution. The linearity of the dilution was validated (S.I. 4).

Table 1: Parameters used on the thermal desorbers (Unity 2 for TD-GC-MS and Unity 1 for TD-PTR-Qi-TOFMS) during sample analysis.

	TD-GC-MS	**TD-PTR-Qi-TOFMS**
Pre-purge time – flow	2.0 min – 20 mL/min	2.0 min – 30 mL/min
Tube desorption time – flow	10.0 min – 20 mL/min	8.0 min – 8 mL/min
Tube desorption temperature	260°C	250°C
Trap low temperature	-10°C	-10°C
Pre-trap fire purge time - flow	2.0 min – 10 mL/min	0.5 min – 8 mL/min
Trap high temperature	280°C	280°C
Trap hold time	3.0 min	3.0 min
Split flow	5 mL/min	40 mL/min
Trap Heating rate	MAX	12 °C/s
Flow Path Temperature	180°C	120°C
Recollection	Yes – on the second tube	No

The reaction conditions in the PTR drift tube are described by the E/N parameter, where E is the electric field along the drift axis and N is the gas number density. It is regulated by the drift tube pressure (p-Drift) and the electric field applied to the drift tube (Udrift). (Lindinger et al., 1998) describes that a compromise should be found to avoid the production of waterclusters (E/N too low, < 120 Td) on the one hand, and fragmentation due to collisions with neutral species (E/N too high, > 150 Td) on the other hand. An E/N value of 144 Td was used during all measurements. Time-integrated data of the time-of-flight mass analyzer was collected every 100 ms. A mass resolution of 5000 m/Δm at m/z = 30 was used. A typical time trace recorded with TD-PTR-Qi-TOFMS is shown in S.I. 11.

2.6 Calibration and data processing

AMDIS (Automated Mass Spectral Deconvolution and Identification System, NIST) was used to run a non-target screening on the obtained TD-GC-MS chromatograms. As a quality control, also a manual screening was performed on the raw chromatographic data, using the mass spectra and the NIST mainlib library for the identification of the major compounds. The set of 54 target compounds was then compiled resulting into a processing method for TD-GC-MS data in Xcalibur 4.2 (Thermo

Scientific) software. Chromatographic peak areas per compound and per sample were obtained. Extracted ion peaks with a signal-to-noise ratio (S/N) lower than 10 were listed as not detected (N.D.). For the PTR-Qi-TOFMS, a data list of m/z ratios (so-called peak table) was generated by processing the entire dataset (stored in the HDF5 data format) using a modified version of the ptairMS package (Roquencourt, 2021; Roquencourt et al., 2022) in R. The selected m/z ratios were crossmatched with a VOC database (Kuo et al., 2020) to annotate the peak table with chemical formulae and remove the masses of isotopes from it. Finally, compounds associated with atmospheric chemistry in clean environments found in the literature were added. PTR-MS Viewer 3 (Ionicon) is used to reprocess the raw PTR data with the obtained peak table and the PTR experimental parameters such as the H_3O^+ concentration, resulting in a corrected CPS trace per m/z ratio. During the thermal desorption step, every time interval (100 ms) a complete mass spectrum (18 – 350 a.m.u.) is recorded. When plotting the intensity (counts per second, CPS) of a selected m/z as a function of time, a right-skewed bell curve profile is obtained. The area under the curve is proportional to the mass of the selected compound in the sample. Peak smoothing and integration are applied to the data in R to finally obtain the corrected peak areas per compound and sample.

In Figure 3, the complete workflow is visualized for both techniques. The relative peak area (RPA) is calculated for each compound per sample by dividing the peak area of the analyte by the peak area of the internal standard (toluene-d8). The method detection limit (MDL) and method quantification limit (MQL) were determined based on the RPA of the target compound present in the three blanks deployed next to the actual sample tubes, i.e. MDL = average(RPA_{blank}) + 3 x stdev(RPA_{blank}) and MQL = average(RPA_{blank}) + 10 x stdev(RPA_{blank}). The MDL and MQL can be expressed as a concentration range (µg/m^3) (Table 3 and S.I. 7) as these values depend on the sampled volume which was determined from the built-in flow measurement. A blank correction is applied to samples by substracting the average response of the compounds in the blank ($RPA_{i,\ corrected} = RPA_i$ – average($RPA_{i,\ blank}$)) to correct for the passive uptake of compounds. The obtained sample mass is divided by the sample volume, to calculate the concentration.

To quantify the compounds, a calibration was performed using an approach as described in (Demeestere et al., 2008). A conditioned sorbent tube was loaded with 1 µL of the calibration solutions (see Section 2.1) and after purging the excess solvent (He, 300 mL, 100 mL/min), it was analyzed using the same methodology as used for the samples. Relative sample response factors (RSRF) for each compound were calculated on both instruments. Results are shown in Table 3. If no RSRF could be determined due to the unavailability of the standards, either the average RSRF of the compound group was used or – for TD-PTR-Qi-TOFMS – the RSRF was assumed to be equal to 1. Since PTR reaction rates are collision-limited, calibration is not strictly necessary and measurements on a PTR-MS without prior calibration are accurate within a factor 2 (de Gouw and Warneke, 2007; Lopez-Hilfiker et al., 2019).

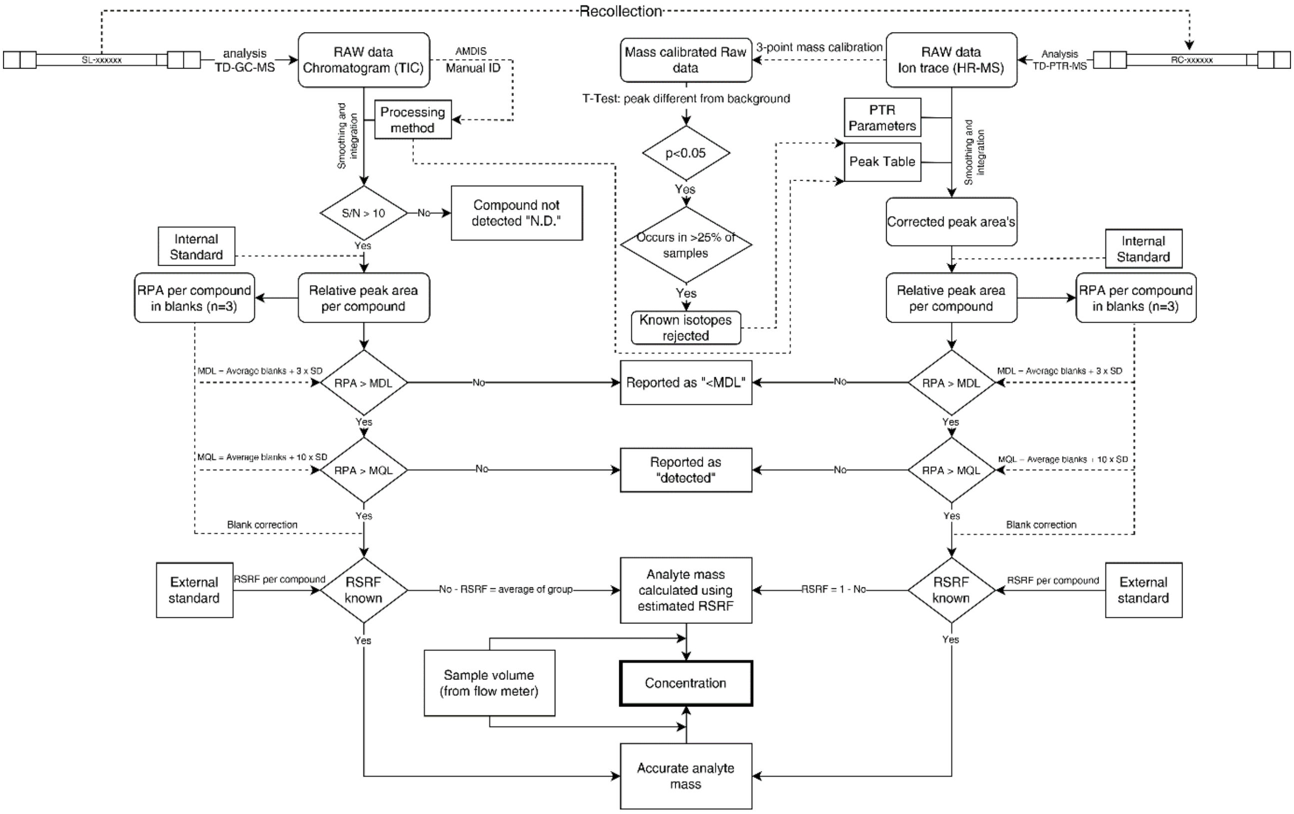

Figure 3: Methodology used to process the data obtained from analyzing the same sample on both TD-PTR-Qi-TOFMS and TD-GC-MS. MDL: Method Detection Limit; MQL: Method Quantification Limit; RSRF: Relative Response Factor; RPA: Relative Peak Area

3 Results and discussion

3.1 Operation of the autosampler

The autosampler was filled with 25 samples and 3 blank sorbent tubes and started sampling on the 12th of December 2019. It completed its pre-programmed schedule of 3 days of sampling followed by 10 days of standby successfully and without user interaction, ending the sampling on 18/10/2020 at position 25. During the campaign, the power supply was interrupted 8 times due to a lack of renewable energy provision or system maintenance, after which the sampler managed to resume its program without intervention. During winter, temperatures reached a minimum of -39 °C and there is no radiative heating from sunlight. This posed extra mechanical and electrical issues. During June and July, the ATS-50 got stuck due to the cold and didn't start sampling in 5 instances. The start and stop dates of each sample, together with the sample volume are listed in **S.I. 9**. The data obtained from the analysis of the 20 successfully sampled sorbent tubes are further discussed in Section 3.3. As the autosampler is effectively a prototype and conditions encountered in Antarctica are extraordinary and difficult to simulate in the lab, some technical issues could be expected. However, as this is the first employment of an autonomous autosampler in Antarctica, its operation is considered very successful and promising for future application.

3.2 Quality control of the analytical approach

At the used sampling volumes, the breakthrough of analytes deserves attention to avoid an underestimation of the actual air concentration. As theoretical or experimental breakthrough volumes of the target analytes are often not available for specific conditions such as air temperatures below 0 °C and lower air density as they occur in Antarctica, an actual in-the-field experiment was conducted. Two standard and identical sorbent tubes (200 mg Tenax TA), prepared as described in Section 2.4, were connected in series with a stainless steel ¼" straight union (Swagelok). In accordance with the samples, 144 L of air was drawn through both tubes using a constant flow pump set at 100 mL/min. The experiment was conducted 6 times during December 2019, in parallel with the use of the autosampler in Antarctica. The sample tubes were analyzed with TD-GC-MS using the methodology described in Section 2.5.1 (without recollection). For each target compound, the ratio of the RPA from the backup tube to the RPA on the front tube was determined. This ratio also represents the mass ratio of the analyte on both tubes. Based on the results shown in S.I. 6, each target compound was categorized into one of 3 groups following the flowchart as shown in S.I. 5. If the total mass of a certain compound on the backup tube is 5% or lower than the front tube, the breakthrough is considered of no concern. This is the case for 39 out of the 56 target compounds. In case the mass ratio is between 5 and 20% (for 2 target compounds), the final air concentration is reported but it must be considered that this is possibly an underestimation of the real concentration. When the mass ratio is higher than 20% (for 15 target compounds), the breakthrough is considered significant, and the calculated concentrations are an underestimation. Therefore, these compounds can be considered as detected but not quantified. Since the experiment took place in December, it is safe to assume that compounds that did not show breakthrough during the summer will also not do so during colder periods as the influence of temperature on the breakthrough volume follows a Van't Hoff-type law (Simon et al., 1995). When a specific VOC was detected in a sample but not during the breakthrough experiment, the theoretical breakthrough volume (BTV) at 0°C was considered if available (www.sisweb.com/index/referenc/tenaxta).

3.3 Occurrence of VOCs in the atmosphere of Dronning Maud Land, East-Antarctica

3.3.1 Halogenated compounds

Brominated and chlorinated compounds participate in ozone depletion in the stratosphere by forming reactive species via photo-dissociation. Nine halogenated species are detected in the samples measured by TD-GC-MS. Bromoform or tribromomethane ($CHBr_3$) is responsible for a large contribution of bromine in the atmosphere and is emitted from the ocean (Quack and Wallace, 2003). It makes it the most prevalent biogenic halogenated methane in Antarctica (Magi and Tanwar, 2014). In our study, bromoform was quantified (above MQL) in 18 out of the 20 samples, and no breakthrough was observed for the used sample volume. Concentrations between 4.6 ng/m³ (14/01/2020) and 23 ng/m³ (01/04/2020) are found (average = 14 ± 6 ng/m³), following a seasonal pattern (Figure 4). During Austral summer, an average of 8 ± 3 ng/m³ is measured. From April on, the air concentration rises steadily to a plateau of 19 ± 2 ng/m³ during April, May, June, July, and August. After this, bromoform again shows a decrease from September on (8.5 ng/m³ on 19/09/2020) which continues with the final 2 samples which are non-quantifiable and not detectable, respectively. (Beyersdorf et al., 2010) found a similar pattern for the bromoform mixing ratio at the South Pole, i.e. a minimum of 0.31 pptv (4.3 ng/m³ at -20°C) during summer and a maximum of 1.28 pptv (15.6 ng/m³ at -20°C) during winter. The slightly higher concentrations in this study are explained by the closer proximity of the sample site to the ocean compared to (Beyersdorf et al., 2010). The seasonal pattern is significantly out of phase with the peak biological activity responsible for bromoform in remote regions. As described in (Beyersdorf et al., 2010), the bromoform input is controlled by the biological activity, sea ice extent and transport efficiency, while its removal is driven by either photolysis (hv) or reaction with $^{\bullet}OH$. As the removal processes only occur in the presence of light, removal during austral winter is expected to be limited. The observed trend suggests a positive influx of atmospheric bromoform during early winter. Other studies (Fischer et al., 2002; Swanson et al., 2004; Wevill and Carpenter, 2004) only measured bromoform during summer and show comparable concentrations (0.3 to 0.6 pptv). For the other eight detected halogenated compounds, breakthrough was observed. Although a fully accurate quantification is not possible, their indicative concentration ranges (i.e. reported values should be interpreted as the minimum concentrations present in the air samples) are given in Table 3.

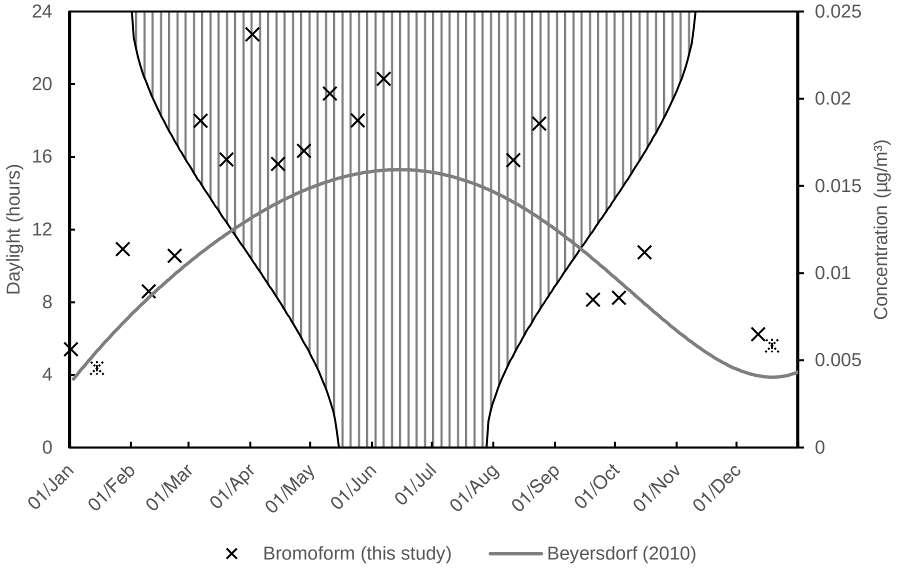

Figure 4: The concentration of bromoform (µg/m³) measured at the PEA station from 2019 to 2020. The shaded area represents the time without sunlight. The Fourier series fit to the data reported by Beyersdorf at South Pole Station is shown by the solid line. Dashed markers indicate the measured value lies below MQL and is substituted by MQL/2 corrected for sample volume.

3.3.2 Non-aromatic hydrocarbons

n-Pentane is the only alkane that is detected by the TD-GC-MS (n=16) and could be quantified in 7 samples. It is highly correlated to anthropogenic activities and natural gas production and has a short lifetime of around 3 days (Bourtsoukidis et al., 2019; Rossabi and Helmig, 2018). Isoprene, which is a biogenic VOC emitted by vegetation and the ocean (Hu et al., 2013), is detected in 14 samples measured by TD-PTR-Qi-TOFMS (0.33 µg/m³ median). Because of the low breakthrough volume, i.e. 50 liters for isoprene (Simon et al., 1996) and 7 liters for n-pentane (Kroupa et al., 2004) for 200mg Tenax TA at -20 °C, no accurate concentrations can be reported. Instead, minimum concentrations are given. Isoprene is only detected on TD-PTR-Qi-TOFMS and is the only non-aromatic hydrocarbon detected by this system. The detection of isoprene suggests that the oceanic influence reaches further than just the coastal regions. During measurements at Toolik Field Station (Alaskan Arctic) in the late spring of 2019, (Selimovic et al., 2022) reported a median concentration of 0.1 µg/m³ for isoprene.

For n-pentane, a median concentration of 0.26 µg/m³ is found which is similar to the concentrations measured by (Gros et al., 1998) during a cruise in the Ross Sea (between 10 and 33 pptv, 0.035 - 0.11 µg/m³), indicating that primary anthropogenic emissions can indeed reach Antarctica in a relatively short time span considering the atmospheric lifetime of n-pentane.

The PTR ionization principle is already extensively discussed by (de Gouw and Warneke, 2007). The soft ionization of the PTR leads to very little or no fragmentation of the parent ion which makes that the analyte is only detected on the accurate mass (in the case of a high-resolution MS) of the compound + H^+. The mass spectra of complex mixtures are significantly simplified by this type of fragmentation and the sensitivity increases. This comes at the cost that compounds with a proton affinity lower than that of water (691 kJ/mol), such as alkanes and most halocarbons, are not ionized and not detectable using PTR-MS. Although fragmentation is assumed to be negligible with PTR, undesirable fragmentation of the mother ion by dissociation remains possible for several compounds. Isoprene and monoterpenes are known to fragment, which causes an underestimation of the real concentration when all fragments are not considered (Schwarz et al., 2009). This effect is represented in Figure 5.

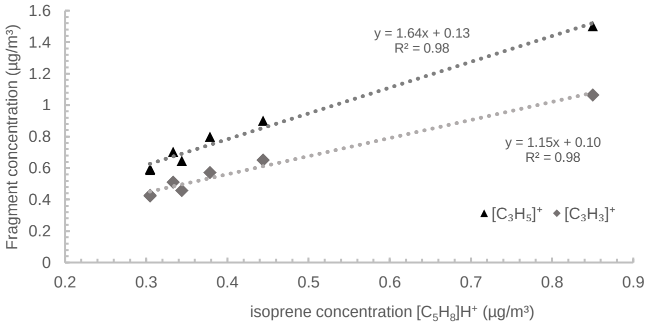

Figure 5: The two main reported fragments originating from the proton transfer reaction of isoprene, $C_3H_5^+$ and $C_3H_3^+$, as a function of the concentration of $[C_5H_8]H^+$ (isoprene) when analyzed by TD-PTR-Qi-TOFMS. A clear linear relation is established indicating that the detected ions are indeed fragments from the isoprene mother ion. The reported isoprene concentrations are not corrected for this fragmentation as no response factors for these fragments are known, thus the shown concentrations should be interpreted with reservation.

3.3.3 Sulfur containing compounds

Sulfur-containing VOCs are of high importance in aerosol particle formation. DMS, which originates mainly from the oceans and is the largest natural source of sulfur in the atmosphere, is detected in 13 samples analyzed by TD-PTR-Qi-TOFMS, but levels were below the quantification limit. This is probably related to the short atmospheric lifetime of 1-2 days and the low breakthrough volume on Tenax TA (Zemmelink et al., 2002). Dimethylsulfone ($DMSO_2$) is a product of the atmospheric oxidation of DMS. (Barnes et al., 2006) suggest the reaction of the OH-DMS-O_2 adduct with HO_2, peroxy radicals, or BrO in NO_x poor and cold conditions to form $DMSO_2$. $DMSO_2$ was measured on both TD-GC-MS (0.26 µg/m³ median, n =16) and TD-PTR-Qi-TOFMS (0.12 µg/m³ median, n = 15). The approximate factor 2 difference can be attributed to interference caused by the neighboring mass peak caused by phenol. The concentrations measured by TD-GC-MS are in agreement with (Edtbauer et al., 2020) who measured $DMSO_2$ using online-PTR-MS during a ship-based measurement in the Arabian sea. Other DMS oxidation products including methanesulfonic acid (MSA), methanesulfinic acid (MSIA), and dimethyl sulfoxide (DMSO) were not detected which is also in line with what (Edtbauer et al., 2020) reported. Methane sulfonyl chloride (MsCl) was identified based on the EI-MS spectrum as well as the TOF-MS spectrum (S.I. 12). The retention time of 21.3 min also supports its identification as, with a Kovats retention index of 741 (Zenkevich, 2005), the compound is expected to elute from the column between n-heptane (t_r = 14.7) and n-octane (t_r = 24.2). No previous data on the atmospheric occurrence of MsCl was found, and neither did we find studies mentioning its formation. Trends observed in both time series (measured by both TD-GC-MS and TD-PTR-Qi-TOFMS) closely match but concentrations obtained by TD-PTR-QiTOF-MS are a factor of 5 lower. This difference could be decreased if MsCl was available as an analytical standard. No significant correlation between the detected sulfur containing compounds was found.

3.3.4 Non-aromatic oxygenated hydrocarbons

Oxygenated VOCs make up the vast majority of compounds detected both in number and mass. A distinction is made between OVOCs containing an aromatic ring structure (n = 32) which will be discussed in Section 3.3.5 and compounds that don't (n = 20). Non-aromatic OVOCs can be formed from aromatic compounds via the photochemical oxidation of aromatic structures via ring-opening mechanisms and by the atmospheric transformation of other VOCs, but also via direct emission by both biogenic and anthropogenic sources. An overview of sources and sinks for the detected non-aromatic OVOCs relevant for a clean environment (i.e. no NO_x chemistry) is listed in Table 2. Half of the 20 detected non-aromatic OVOCs were only detected using TD-PTR-Qi-TOFMS analysis. Glyoxal was only detected by TD-GC-MS (0.04 µg/m³ median). Methylglyoxal (0.11 µg/m³ median), maleic anhydride (0.08 µg/m³ median), and butenedial and 2-furanone ($(C_4H_4O_2)H^+$ 0.03 µg/m³ median) are only detected using TD-PTR-Qi-TOFMS. The aforementioned compounds are known atmospheric oxidation products of toluene formed via the peroxy-bicyclic ring opening mechanism described in detail by (Bloss et al., 2005).

Table 2: Examples of atmospheric sources and transformation products found in the measurement of oxygenated hydrocarbons. Only reactions that can occur in a clean environment (NOx limited) are considered. To simplify the table, only transformation products that were detected during the measurement are listed. For all compounds, further oxidation by •OH is a significant sink, together with removal by dry and/or wet deposition. 1 (Bloss et al., 2005), 2 (Fu et al., 2008), 3 (Gilman et al., 2015),4 (Coggon et al., 2019), 5 (Y. Yuan et al., 2017), 6 (Franco et al., 2021), 7 (Warneck, 2005), 8 (Villanueva et al., 2009), 9 (Kesselmeier et al., 2000), 10 (Eger et al., 2020), 11 (Calvert et al., 2002), 12 (Stockwell et al., 2015)

Compound	**Atmospheric source**	**Transformation products**	**Found by** (Ciccioli et al., 1996b)
Glyoxal	Oxidation of aromatics via phenol and photolysis butenedial [1] and oxidation of isoprene [2]		
Furan	Biomass Burning [3]	furanones and butenedial [4], maleic anhydride [5]	
Formic acid	Formaldehyde via multiphase transformation [6]		
n-Butanal			X
2-butanone			X
Acetic Acid	•OH + acetone, OH_2 radical + acetyl peroxy, propene + O_3 [7]		X
Hexanal	oxidation C_6		X
Butyric Acid			X
2-Furaldehyde	oxidation of methylfuran [8], biomass burning		
Octanal	oxidation C_8		X
Acrolein	photolysis butenedial (+CO) [1]		
Methacrolein + Methyl vinyl ketone	oxidation of isoprene [9]	Pyruvic acid[10]	MVK
Methylglyoxal	Oxidation of aromatics [1] and isoprene		
Propanoic Acid			X
2-Methylfuran	oxidation of isoprene [9] + biomass burning[3,8]	2-furaldehyde [8], maleic anhydride [4]	X
Butenedial	oxidation toluene (peroxy bicyclic ring opening) [1]	glyoxal, maleic anhydride, acroleine [1]	
2-Furanone	photolysis butenedial and oxidation aromatics [1]		
Biacetyl	Oxidation of xylenes and trimethylbenzenes [11]		
Pentanal + 2-Pentanone	oxidation Pentane/Pentanol and biomass burning[12]		X
Pyruvic acid	Ozonolysis MVK and photolysis methylglyoxal [10] C_3 carbonyls via multiphase transformation[6]		
Maleic Anhydride	photolysis butenedial [1]		

Organic acids (n=5) are ubiquitous in the samples, with formic acid being the most prevalent of the non-aromatic acids found. It is measured with both instruments but a lower concentration was found with TD-PTR-Qi-TOFMS (0.47 µg/m^3 compared to 2.02 µg/m^3 median), which is probably related to the aberrant peak shape of formic acid on the GC. (Franco et al., 2021) proposed the multiphase pathway to convert formaldehyde to formic acid via methanediol in cloud water, and also suggested an equivalent process for the formation of oxalic acid and pyruvic acid from C_2 and C_3 carbonyls. A similar concentration (0.62 µg/m^3) for formic acid was reported by (Selimovic et al., 2022) in the Arctic. For none of the non-aromatic acids in Table 3, a clear seasonal trend could be observed, i.e. concentrations seem to remain constant around their median value, i.e. 1.33 µg/m^3 for acetic acid which was only detected with TD-GC-MS, 0.13 µg/m^3 for butyric acid measured on TD-GC-MS compared to 0.15 µg/m^3 using TD-PTR-Qi-TOFMS, and 0.20 µg/m^3 for propanoic acid which was only measured by TD-PTR-Qi-TOFMS. For the other non-aromatic oxygenated compounds such as 2-furaldehyde (0.02 µg/m^3 and 0.05 µg/m^3 median for TD-GC-MS and TD-PTR-Qi-TOFMS respectively) and furan (0.09 µg/m^3 and 0.06 µg/m^3 median for TD-GC-MS and TD-PTR-Qi-TOFMS), a seasonal pattern can be observed which in fact is best shown as a function of the number of sunlight hours during the time at which the specific sample was taken. Concentration sensitivity to sunlight indicates oxidation by $^{\bullet}$OH is an important removal pathway. As shown in Figure 6, an inverse linear relation is established, and the model is verified to be a good fit with a 99% confidence interval to the data using regression analysis.

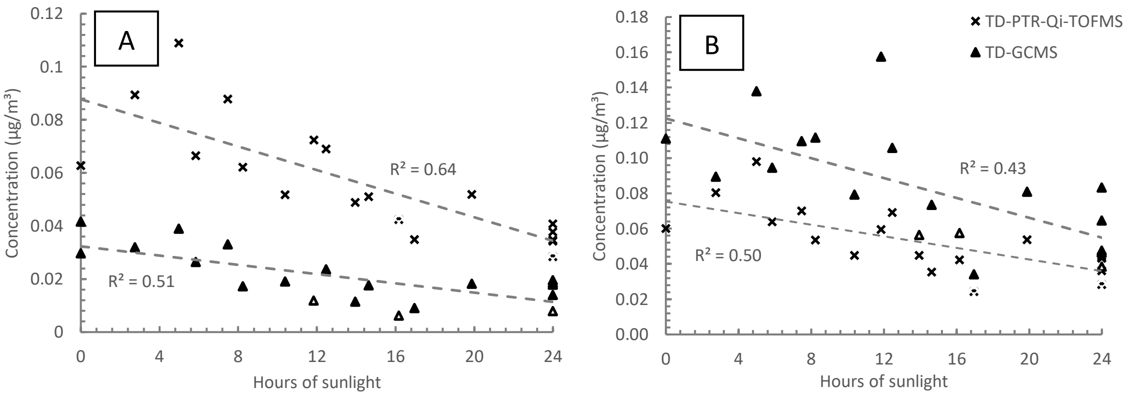

Figure 6: Trend of 2-furaldehyde (A) and furan (B) measured by TD-GC-MS and TD-PTR-Qi-TOFMS, respectively, as a function of the average amount of daylight at the time of sampling. Hours of sunlight are calculated according to the sunrise equation for the measurement location (see SI). The indicated trends are significant with a 99% CI. Greyed-out points are below MQL, MQL/2 corrected for sample volume was used to substitute the value.

Although atmospheric oxidation processes are very complex, and despite that, some of the parent/product relationships described in Table 2 are simplified, some compounds are rather directly formed from another. Two examples are highlighted in Figure 7. Acrolein (median 0.08 µg/m³) is a possible product of butenedial (median 0.03 µg/m³) formed via photolysis (Bloss et al., 2005). Both compounds show a similar pattern over time confirming their relation. Furaldehyde (median 0.05 µg/m³) is reported by (Villanueva et al., 2009) to be formed from 2-methylfuran in the presence of chlorine atoms. A particular pattern is observed for these 2 compounds over time. During the summer months (December, January), concentrations for both compounds were established as nearly identical. From February on and through winter, a strong discrepancy is observed in the sense that 2-furaldehyde concentrations are more than a factor of 2 higher. This indicates either an influx of 2-furaldehyde from another source such as biomass burning (Koppmann, 2007), although no significant rise of biomass burning tracers such as benzonitrile or phenylacetylene is observed, or that the removal of 2-furaldehyde is limited from early winter on while its production is continued via chlorine chemistry. Despite knowledge on chlorine chemistry in polar regions is still evolving, reactive chlorine is expected to be available during winter via chlorine recycling and liberation from sea salt particles (Hara et al., 2002).

When compared to the Arctic, very similar concentrations are found for the reported OVOCs. (Selimovic et al., 2022) report median values of 0.044, 0.08, 0.014, 0.011 and 0.04 µg/m³ for acrolein, methacrolein, methylfuran, butenedial and 2-furaldehyde, though for furan (median 0.006 µg/m³,) and maleic anhydride (median 0.013 µg/m³) larger differences are established.

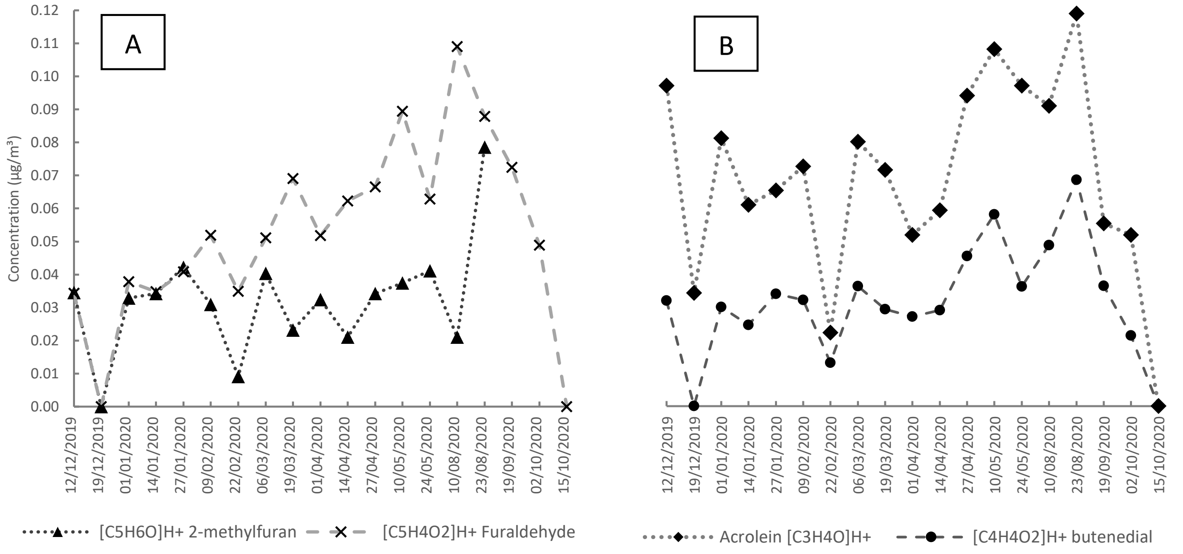

Figure 7: The relationship between concentrations of selected non-aromatic OVOCs over time. Ordinate has the same scale for both figures.

3.3.5 Aromatic compounds

Benzene (C_6H_6) is the simplest aromatic hydrocarbon and arises from primarily anthropogenic sources. At $^\bullet OH$ levels encountered in Antarctica (between 1 and 5 x 10^5 molecules.cm^{-3} (Bloss et al., 2007)), the atmospheric lifetime of benzene is estimated between 17 days in summer and 89 days in winter (reaction rate $k_2 = 1.3 * 10^{-12}$ cm^3.molecules^{-1}.s^{-1} at 263 K, iupac.aeris-data.fr). Its long lifetime (Read et al., 2007) enables the compound to be transported over long distances. Theoretical and experimental atmospheric lifetimes considering only summer conditions are given for all compouds discussed in this study in **S.I. 8**. (Verreyken et al., 2020) showed that biomass burning caused an enhancement in benzene concentrations in the remote atmosphere of La Réunion. During our measurement campaign in Antarctica, concentrations between 75 ng/m^3 (10/08/2020) and 29 ng/m^3 (6/3/2020) were found. These values (median = 40 ng/m^3) are based on the TC-GC-MS analysis. The concentrations of benzene measured on TD-PTR-Qi-TOFMS are significantly higher (median = 0.88 µg/m^3). At the used drift tube conditions, the mother ion of ethylbenzene dissociates which results in an ion interfering with the mass of $[C_6H_6]H^+$ (benzene) (Gueneron et al., 2015). Though the measured minimum and maximum concentrations suggest a seasonal pattern, no significant trend is observed. The measured values highly resemble earlier measurements in Antarctica by (Beyersdorf et al., 2010) who found values between 4 and 15 ppt$_v$ (15 and 56 ng/m^3 at -20°C), and (Read et al., 2007) who also found a minimum during summer of 1.5 ppt$_v$ (5.5 ng/m^3) and a maximum of 17.6 ppt$_v$ (64 ng/m^3) which occurred during winter.

Toluene, ethylbenzene, and the xylene isomers were measured by (Rudolph et al., 1992b) near the McMurdo station at concentrations sometimes exceeding 10 ppt$_v$ (0.044 µg/m^3). These relatively high levels were determined to be caused by contamination from the station. As our measurements took place close to the PEA station, a comparable observation is made. During the 2019-2020 expedition, the station was inhabited until 25/02/2020 which is clearly reflected in the data. During the first 7 samples, up until 22/02/2020, concentrations were a factor of 10 higher compared to the period later than 06/03/2020 when the station was not inhabited. During the first period, average concentrations for toluene, m/p-xylene, and ethylbenzene were 71 (±67), 34 (±34), and 10 (±10) ng/m^3, respectively, while during the second period 9.0 (±3.3), 2.1 (±0.9) and 1.1 (±0.1) ng/m^3 was measured and concentrations dropped frequently below MQL. For the first 7 samples, the concentrations of these compounds show a similar pattern suggesting a common source, such as vehicular emissions. Toluene is often used to evaluate the performance of VOC analysis techniques. As shown in Figure 8, very good correlation is found for the toluene concentrations measured with both techniques. While the mixing ratios of benzene, ethylbenzene, toluene, and xylene are enhanced by local emissions, three non-oxygenated aromatic compounds are detected by TD-GC-MS for which no correlation between the occupation of the station and the measured level is found. Ethynylbenzene (phenylacetylene) and benzonitrile were found at concentrations between 12 and 36 ng/m^3, and between 4 and 9 ng/m^3, respectively. Styrene was under the quantification limit in all samples but was detected in 8 samples. The three mentioned compounds are related to biomass burning according to previous studies (Gilman et al., 2015; Koss et al., 2018; Stockwell et al., 2015), strongly indicating the influx of contaminated air masses.

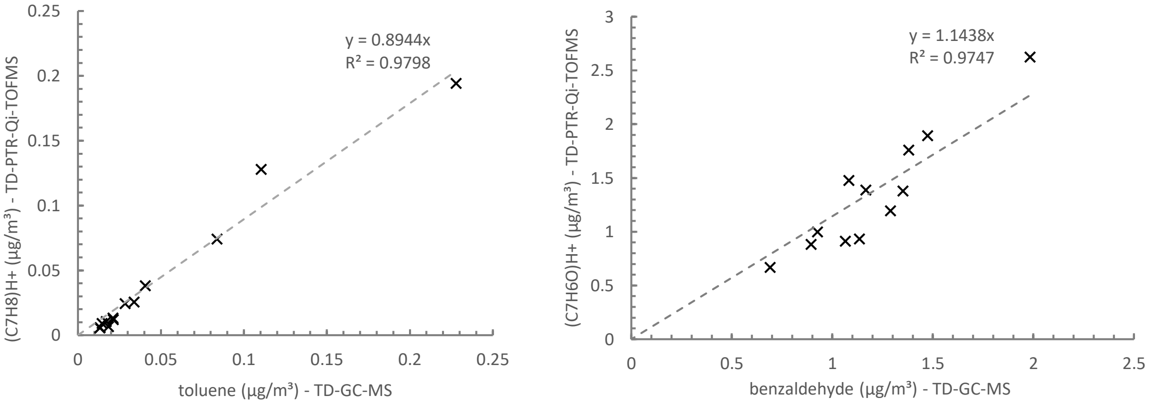

Figure 8: X-Y correlation plots for toluene (left) and benzaldehyde (right) concentrations, measured with both TD-GC-MS and TD-PTR-Qi-TOFMS.

Next, 24 oxygenated compounds containing an aromatic ring structure and associated with biomass burning and photochemical oxidation, are detected and quantified. Benzaldehyde is formed by the H-abstraction of the methyl group of toluene with an $^{\bullet}$OH radical, then a secondary oxidation to benzoic acid is possible. (Salta et al., 2020) suggest several pathways via the benzyl radical which lead to the formation of benzoic acid as the foremost oxidation product. Both compounds are amongst the most prevalent oxygenated aromatics measured in our study. Benzaldehyde is found at concentrations between 0.69 and 1.98 µg/m³ (1.13 µg/m³ median) on the TD-GC-MS which resembles the concentrations measured by (Ciccioli et al., 1996b) near Terra Nova Bay (0.23 – 1.08 µg/m³). For the TD-PTR-Qi-TOFMS measurement similar concentrations are found, between 0.68 and 2.862 µg/m³ (1.2 µg/m³ median) and good correlation with the TD-GC-MS data was established (Figure 8). Concentrations of benzoic acid, measured on TD-GC-MS, are a factor of 10 higher, ranging between 4.73 and 20.3 µg/m³ (11.0 µg/m³ median). No experimental RRF could be determined for benzoic acid, so the average RRF within the group was used, which could introduce a systematic error. This is expected to be limited since TD-PTR-Qi-TOFMS measurements of benzoic acid provided slightly lower but similar concentration values (8.15 µg/m³ median). An interesting observation is the very strong correlation between the level of benzaldehyde and benzoic acid (Figure 9a) indicating a common source.

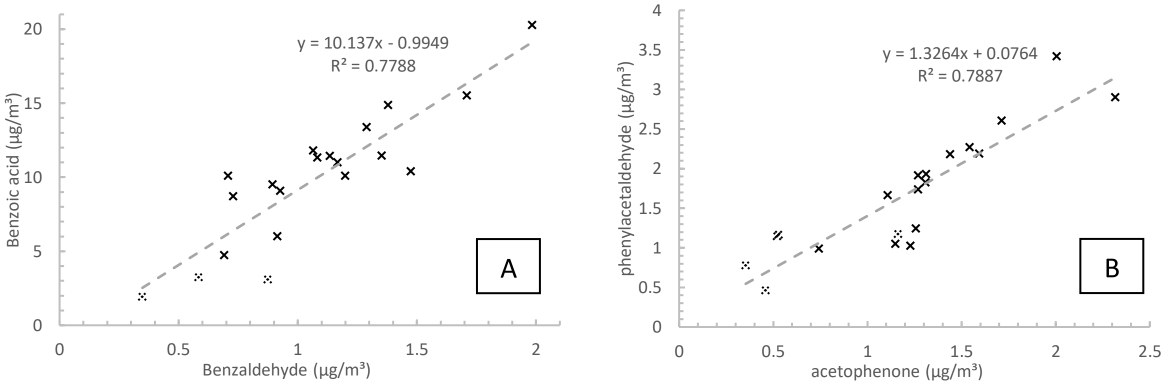

Figure 9: Measured air concentration levels for oxidation products of toluene, benzoic acid and benzaldehyde (figure A) measured by TD-GC-MS and oxidation products of ethylbenzene, phenylacetaldehyde and acetophenone (figure B) measured by TD-GC-MS. Values below the detection or quantification limit were substituted by MDL/2 and MQL/2 corrected for the sample volume (greyed out crosses).

(Salta et al., 2020) also found phenol and p-benzoquinone as possible oxidation products of toluene. P-Benzoquinone was detected in all samples but did not show any significant relation with structurally related compounds. Phenol is also readily formed form the reaction of O_2 with the OH-benzene adduct (Atkinson and Arey, 2003). Despite this, phenol did not show a good correlation with the air concentration of benzene, though this is probably due to the low levels of benzene which are close to the MQL for all samples.

Acetophenone and phenylacetaldehyde are both oxidation products of ethylbenzene. Though phenylacetaldehyde has never been detected in situ as a product during photooxidation studies in laboratories, (Xu et al., 2003) proved that phenylacetaldehyde is a product of the (ethylbenzene + $^{\bullet}$OH) reaction by hydrogen atom abstraction from the ethyl group in the presence of O_2 and NO_x. Figure 9b shows a significant (ANOVA, 99% C.I.) linear relation for the concentration of acetophenone (0.74 – 2.32 µg/m³, measured by TD-GC-MS) and phenylacetaldehyde (1.67 – 3.42 µg/m³, also measured by TD-GC-MS) indicating a common primary source, likely ethylbenzene. It is noted that the ratio between the two compounds is almost unity, which differs from what the authors found in Greece (Xu et al., 2003). Since ethylbenzene concentrations were enhanced by local emissions, it is impossible to find acetophenone/ethylbenzene and phenylacetaldehyde/ethylbenzene concentration ratios similar to the previously mentioned study. The alteration of compound ratios is more significant during the much longer transport times, between 10 and 30 days from the source to Antarctica, compared to the photochemical age of 0.75-2.5 days found by (Xu et al., 2003).

Although the lack of a chromatographic separation step does significantly shorten the analysis time with TD-PTR-Qi-TOFMS, the measurements of acetophenone and phenylacetaldehyde exemplify the added value and compatibility of both analytical techniques. With TD-PTR-Qi-TOFMS, isomeric compounds contribute to the same signal as their exact masses are identical. In such cases, a chromatographic separation by GC is an added value, enabling the quantification of individual isomers, as illustrated in Figure 10 for acetophenone and phenylacetaldehyde.

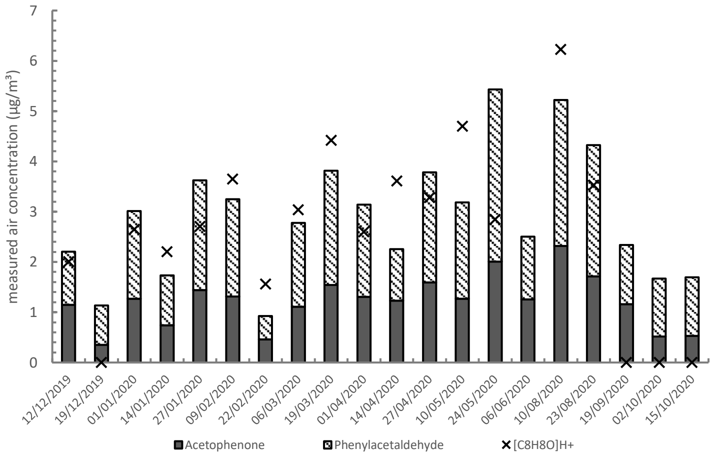

Figure 10: Two isomers, acetophenone and phenylacetaldehyde, measured as individual components on TD-GC-MS compared to the concentration obtained from the accurate mass (m = 121,06479 – $(C_8H_8O)H^+$) on TD-PTR-Qi-TOFMS.

Table 3: General overview of all compounds detected in the samples analyzed by both TD-GC-MS and TD-PTR-Qi-TOFMS. # = number of instances detected, * = possible breakthrough †= isomers

Compound	CAS	Formula	MW	TD-GC-MS				Concentration				TD-PTR-MS			Concentration			
				t_R min.	MS ions	MDL µg/m³	MQL µg/m³	Median µg/m³	min µg/m³	max µg/m³	# n=20	MH+	MDL µg/m³	MQL µg/m³	Median µg/m³	min µg/m³	max µg/m³	# n=19
Non-aromatic Hydrocarbons																		
n-Pentane*	109-66-0	C_5H_{12}	72.15	3.75	39;42;43;57;72	0.01-0.03	0.02-0.06	0.03	0.02	0.07	16							
n-Hexane*	110-54-3	C_6H_{14}	86.18	7.05	41;71;86	0.05-0.13	0.1-0.27	4.05	0.27	7.82	3							
Isoprene	78-79-5	C_5H_8	68.12									69.0699	0.14-0.37	0.32-0.85	0.33	0.17	0.84	14
Halogenated compounds																		
Trichloromonofluoromethane (Freon 11)*	75-69-4	CCl_3F	137.37	3.42	101;103;105	0.38-1.01	0.58-1.52	<LOQ	0.00	0.00	3							
1,1,2-trichloro-1,2,2-trifluoroethane (Freon	76-13-1	$C_2Cl_3F_3$	187.38	4.35	101;103;151;153	2.7-7.15	4.57-12.09	<LOQ	0.00	0.00	1							
Methylene chloride (Freon-30)*	75-09-2	CH_2Cl_2	84.93	4.28	49;84;86	0.01-0.02	0.01-0.03	0.0090	0.0028	0.020	13							
Trichloromethane (Freon 20)*	67-66-3	$CHCl_3$	119.38	7.4	47;83;85	0.03-0.07	0.04-0.11	0.026	0.026	0.026	11							
1,2-dichloroethane (Freon 150)*	107-06-2	$C_2H_4Cl_2$	98.95	8.72	62;98	0.01-0.02	0.01-0.03	0.006	0.005	0.011	14							
1,1,1-trichloroethane (Freon 140a)*	71-55-6	$C_2H_3Cl_3$	133.4	9.3	97;99;117;119	0.02-0.04	0.02-0.06	0.012	0.011	0.014	10							
Carbon Tetrachloride (Freon-10)*	56-23-5	CCl_4	153.82	10.7	117;119;121	0.77-2.03	1.16-3.08	<LOQ	0.00	0.00	9							
Tribromomethane	75-25-2	$CHBr_3$	252.75	27.85	171;173;175	0.01-0.02	0.01-0.02	0.016	0.005	0.024	18							
Bromomethane*	74-96-4	CH_3Br	94.94	2.7	94;96	0.001-0	0.002-0.01	<LOQ	0.000	0.000	16							
Sulfuric compounds																		
Dimethylsulfide	75-18-3	C_2H_6S	62.13									63.0263	0-0.01	0.01-0.02	<LOQ	0.000	0.000	13
Methanesulfonyl Chloride	124-63-0	CH_3ClO_2S	114.54	21.25	79;99	0.03-0.09	0.07-0.18	0.12	0.07	0.19	17	114.9615	0.01-0.02	0.01-0.04	0.02	0.01	0.04	17
Dimethylsulfone	67-71-0	$C_2H_6O_2S$	94.13	28	45;94	0.08-0.22	0.14-0.36	0.26	0.08	0.53	16	95.0161	0.05-0.14	0.08-0.22	0.12	0.05	0.24	15
OVOCs (non-aromatic)																		
Glyoxal	107-22-2	$C_2H_2O_2$	58.04	2.4	31:44:58	0.01-0.02	0.02-0.05	0.04	0.02	0.07	18	59.0128						
Furan	110-00-9	C_4H_4O	68.08	3.68	68;69	0.02-0.06	0.04-0.11	0.09	0.03	0.16	20	69.0335	0.03-0.07	0.05-0.14	0.06	0.04	0.10	18
Formic acid	64-18-6	CH_2O_2	46.03	4.5	29;45;46	0.43-1.14	1.01-2.66	2.02	1.16	3.47	19	47.0128	0.11-0.28	0.2-0.52	0.47	0.24	0.84	18
n-Butanal*†	123-72-8	C_4H_8O	72.11	5.95	43;57;72	0.02-0.04	0.02-0.06	0.12	0.04	0.27	19	73.0648	0.04-0.1	0.06-0.15	0.04	0.03	0.06	18
2-butanone*†	78-93-3	C_4H_8O	72.11	6.15	43;72;73	0.03-0.08	0.05-0.12	0.05	0.03	0.09	18	73.0648						
Acetic Acid	64-19-7	$C_2H_4O_2$	60.05	7.15	43;45;60	0.66-1.76	1.37-3.64	1.33	1.26	1.41	16	61.0284	0.9-2.39	1.74-4.61	<LOQ	0.00	0.00	13
Hexanal*	66-25-1	$C_6H_{12}O$	100.16	22.5	44;56;57;72;82	0.05-0.14	0.13-0.34	0.19	0.13	0.43	14	101.0961						
Butyric Acid	107-92-6	$C_4H_8O_2$	88.11	23.9	60;73	0.03-0.08	0.05-0.14	0.13	0.05	0.39	16	89.0597	0.05-0.14	0.09-0.24	0.15	0.07	0.26	17
2-Furaldehyde	498-60-2	$C_5H_4O_2$	96.09	24.6	95;96	0-0.01	0.01-0.02	0.02	0.01	0.04	19	97.0284	0.03-0.07	0.05-0.13	0.05	0.04	0.12	15
Octanal	124-13-0	$C_8H_{16}O$	128.21	32.25	41,43,56,57	0.11-0.29	0.27-0.7	0.37	0.24	1.21	15	129.1274	0.01-0.02	0.01-0.04	0.02	0.01	0.05	15
Acroleine*	107-02-8	C_3H_4O	56.06									57.0335	0.05-0.12	0.08-0.2	0.08	0.05	0.12	18
Methacrolein	78-85-3	C_4H_6O	70.09									71.0491	0.02-0.06	0.03-0.08	0.04	0.02	0.10	18
Methylglyoxal	78-98-8	$C_3H_4O_2$	72.06									73.0284	0.03-0.09	0.07-0.18	0.11	0.07	0.14	18
Propanoic Acid	79-09-4	$C_3H_6O_2$	74.08									75.0441	0.12-0.32	0.24-0.65	0.20	0.19	0.21	16
2-Methylfuran	534-22-5	C_5H_6O	82.1									83.0491	0.01-0.02	0.01-0.03	0.03	0.01	0.08	18
Butenedial	2363-83-9	$C_4H_4O_2$	84.07									85.0284	0.02-0.04	0.03-0.08	0.03	0.02	0.07	17
Biacetyl	431-03-8	$C_4H_6O_2$	86.08									87.0441	0.05-0.12	0.1-0.27	<LOQ	0.00	0.00	14
Pentanal/2-Pentanone	110-62-3/107-87-9	$C_5H_{10}O$	86.13									87.0804	0.01-0.04	0.02-0.05	0.03	0.01	0.04	16
Pyruvic acid	127-17-3	$C_3H_4O_3$	88.06									89.0233	0-0.01	0.01-0.02	0.00	0.00	0.01	15
Maleic Anhydride	108-31-6	$C_4H_2O_3$	98.06									99.0077	0.04-0.09	0.08-0.21	0.08	0.07	0.08	15
Aromatic compounds																		
Benzene	71-43-2	C_6H_6	78	10.5	52:63:77:79	0.04-0.1	0.06-0.15	0.040	0.030	0.070	16	79.0542	0.31-0.82	0.68-1.79	0.88	0.66	1.67	18
Toluene	108-88-3	C_7H_8	92	20.1	65;91;92	0.01-0.02	0.01-0.03	0.014	0.005	0.194	18	93.0699	0.02-0.05	0.03-0.07	0.02	0.01	0.23	18
Ethylbenzene†	100-41-4	C_8H_{10}	106.17	27.2	91.0;106	0.001-0.002	0.001-0.003	0.003	0.001	0.027	17	107.0855			Fragmentation			
m-xylene†	108-38-3	C_8H_{10}	106.17	27.62	91;105;106	0.001-0.002	0.001-0.003	0.003	0.001	0.094	18	107.0855	0.25-0.65	0.51-1.34	0.52	0.52	0.52	16
Phenylacetylene	536-74-3	C_8H_6	102.14	27.8	102;103	0.01-0.02	0.01-0.04	0.020	0.012	0.036	16	103.0542	0.03-0.08	0.05-0.14	0.07	0.06	0.10	17
Styrene	100-42-5	C_8H_8	104	28.5	51;78;104	0.002-0.006	0.004-0.01	<LOQ	0.000	0.000	8	105.0699						
p-Benzoquinone	106-51-4	$C_6H_4O_2$	108	28.6	80;82;108;110	0.03-0.08	0.03-0.09	0.040	0.010	0.094	20	109.0284	0.03-0.07	0.05-0.13	0.05	0.03	0.08	17
o-xylene	95-47-6	C_8H_{10}	106.17	28.7	91;105;106	0.001-0.001	0.001-0.002	0.001	0.000	0.034	18	107.0855			isomer of m-xylene and ethylbenzene			
Benzaldehyde	100-52-7	C_7H_6O	106	30.85	77;105;106	0.5-1.32	0.67-1.76	1.134	0.690	1.983	20	107.0491	0.94-2.5	1.34-3.55	1.20	0.67	2.62	18
Benzonitril	100-47-0	C_7H_5N	103	31.45	76;103	0.003-0.009	0.005-0.013	0.005	0.004	0.009	18	104.0495	0.007-0.018	0.009-0.024	0.005	0.004	0.009	17
Phenol	108-95-2	C_6H_6O	94.11	31.85	66,94	0.2-0.54	0.24-0.63	0.629	0.109	1.058	19	95.0491	0.5-1.32	1.01-2.68	0.92	0.77	1.41	16
Benzofuran	271-89-6	C_8H_6O	118.14									119.0491	0-0.01	0-0.01	0.01	0.00	0.01	18
Phenylacetaldehyde†	122-78-1	C_8H_8O	120.15	33.35	69;91;120	0.89-2.35	1.99-5.26	2.187	1.666	3.424	15	121.0648			isomer of acetophenone			
3-hydroxybenzaldehyde†	100-83-4	$C_7H_6O_2$	122.12	33.54	65;93;121;122	0.31-0.83	0.66-1.75	0.772	0.568	1.329	16	123.0441			isomer of benzoic acid			
Propoxybenzene	622-85-5	$C_9H_{12}O$	136.2	33.87	66;94;136	0.001-0.003	0.002-0.006	0.003	0.002	0.004	16	137.0961	-		-	-	-	-
Acetophenone†	98-86-2	C_8H_8O	120.15	34.1	61;77;105;120	0.4-1.07	0.88-2.33	1.309	0.742	2.317	17	121.0648	1.32-3.49	2.81-7.45	3.04	1.56	6.23	17
Phenylglyoxal†	1074-12-0	$C_8H_6O_2$	134.13	34.3	77;105;121	0.23-0.6	0.55-1.46	1.699	0.582	3.409	18	135.0441	0.15-0.39	0.33-0.88	0.49	0.34	0.97	16
Methylbenzoate†	93-58-3	$C_8H_8O_2$	136.15	34.9	77;105;121	0.001-0.002	0.001-0.003	0.003	0.001	0.007	20	137.0597	0.01-0.04	0.03-0.08	0.03	0.02	0.05	17
1,3-Benzodioxol-2-one	2171-74-6	$C_7H_4O_3$	136.11	35.5	63;64;92;136	0.004-0.011	0.01-0.03	0.015	0.009	0.029	17	137.0233	0.01-0.03	0.03-0.07	0.03	0.02	0.04	17
Benzoic acid†	65-85-0	$C_7H_6O_2$	122.12	37.1	77;105;135	2.36-6.25	3.71-9.83	11.002	4.732	20.281	19	123.0441	0.92-2.43	2.43-6.19	8.15	2.93	13.64	18
2-Coumaranone†	553-86-6	$C_8H_6O_2$	134.13	37.9	78;105;122;134	0.03-0.07	0.06-0.16	0.066	0.053	0.096	17				isomer of phenylglyoxal			
2-hydroxyacetophenone†	118-93-4	$C_8H_8O_2$	136.15	38.1	51;77;105	0.01-0.03	0.02-0.06	0.233	0.024	0.380	19	137.0597		isomer of Phenylacetic acid + methylbenzoate				
Phenylacetic acid†	103-82-2	$C_8H_8O_2$	136.15	38.2	65;91;136	0.03-0.08	0.07-0.18	0.107	0.075	0.168	17	137.0597		isomer of 2-hydroxyacetophenone + methylbenzoate				
Benzoylformic acid	611-73-4	$C_8H_6O_3$	150.14	38.9	51;77;105	0.003-0.007	0.01-0.02	0.186	0.005	0.494	18	151.0390	0.01-0.02	0.01-0.03	0.01	0.01	0.02	18
2,3-Benzofurandione	4732-72-3	$C_8H_4O_3$	148.12	39	63;64;92;120	0.09-0.23	0.16-0.41	0.603	0.123	1.310	19	149.0233	0.14-0.36	0.26-0.68	0.207	0.207	0.207	11
Phtalic acid	88-99-3	$C_8H_6O_4$	166.13	39.2	76;104;105;148	0.45-1.19	0.94-2.5	<LOQ	0.000	0.000	2	167.0339	0.01-0.03	0.02-0.05	<LOQ	0.000	0.000	16
2-ethoxybenzaldehyde	613-69-4	$C_9H_{10}O_2$	150.17	40.2	105;121;122;150	0.002-0.004	0.004-0.011	0.024	0.011	0.074	17	151.0754						
Phenylmaleic anhydride	36122-35-7	$C_{10}H_6O_3$	174.15	42.2	102;174	0.95-2.51	2.21-5.85	2.386	2.177	2.595	17	175.0390	0.19-0.5	0.52-1.37	0.606	0.482	0.717	17
Benzophenone	119-61-9	$C_{13}H_{10}O$	182.22	43.9	77;105;182	0.04-0.1	0.08-0.22	0.125	0.080	0.199	18	183.0804	0.02-0.05	0.03-0.08	0.024	0.016	0.040	18
Benzoic acid phenyl ester	93-99-2	$C_{13}H_{10}O_2$	198.22	44.3	77;105;198	0.01-0.03	0.03-0.08	0.040	0.027	0.071	18	199.0754	0.01-0.02	0.01-0.02	0.019	0.010	0.030	18
1,2-diphenyl Ethanone	451-40-1	$C_{14}H_{12}O$	196.25	45.5	77;105;196	0.11-0.29	0.25-0.65	0.231	0.224	0.238	17	197.0961	0-0	0-0	0.008	0.005	0.013	11

4 Conclusions and future prospect

A dedicated autosampler capable of taking multiple samples in an extreme environment such as Antarctica was developed in-house and deployed from December 2019 to October 2020 in Dronning Maud Land, East-Antarctica. This led to, for the first time, a year-round dataset of 66 VOCs reported for East-Antarctica and marks the first time that these compounds were successfully sampled in an automated sequential manner in Antarctica for later, off-line analysis. Sorbent tubes were used because of their robustness and since they combine sampling and sample preparation in one step. An in-situ breakthrough experiment was conducted to determine which compounds are sensitive to breakthrough. A main benefit of the novel autosampler is that it allows gaining temporal information on VOCs in regions where it is difficult to install and maintain an on-line measurement. Furthermore, this method is significantly cheaper compared to the alternatives such as online-GC and allows researchers to simultaneously run a measurement on several sites and then analyze the samples in a centralized laboratory, significantly increasing the amount of data available on VOCs and atmospheric oxidation products. Samples were analyzed using the more traditional TD-GC-MS and a novel technique encompassing a high-resolution PTR-Qi-TOFMS which was interfaced to a thermal desorber (TD-PTR-Qi-TOFMS). Characteristics of both instruments were compared and both techniques are found to be very complementary. While a good correlation was found between the concentrations of most compounds reported with both instruments, each proved to have its own advantages and drawbacks. The chromatographic separation of a GC proves to be a necessity to separate isomers (e.g., acetophenone and phenylacetaldehyde, being atmospheric oxidation products of ethylbenzene) and an EI-MS is capable of detecting alkanes and halocarbons. On the other hand, the alternative soft ionization source of the TD-PTR-Qi-TOFMS enabled to extend the range of measured analytes and the detection of some specific compounds such as DMS and 10 OVOCs related to atmospheric chemical processes which are rarely reported. Although the online capability of the PTR-Qi-TOFMS instrument was sacrificed to interface it with a thermal desorber for increased sensitivity, it still performs a fourfold faster compared to GC-MS, and the high-resolution MS adds an extra possibility for the screening of non-target compounds. The combination of both techniques and the non-target approach led to a very diverse dataset, spanning across different groups of organic compounds (aromatic, halocarbons,…), from very reactive to very persistent, and molecular weights from 46 to 253 g/mol. Concentration ranges from 0.5 ng/m³ (methylbenzoate) to 20 µg/m³ (benzoic acid) were found. Almost half (n=32) of the detected species in the samples are oxygenated compounds. Some (furaldehyde, furan) show clear trends as a function of the amount of daylight. From literature, OVOCs could be identified as products from different atmospheric oxidation processes. Furthermore, several parent compounds (e.g. isoprene, toluene), as well as very advanced oxidation products (glyoxal), were found.

Through the development of a novel and robust sequential autosampler, and by using both instrumental analytical methods, year-round concentrations of 66 VOCs and atmospheric oxidation products were established, providing insight into the atmospheric chemistry in Antarctica. With this unique dataset, we contribute to a scientific domain where in-situ collected data is very sparse. The developed technique offers potential to further investigate the atmospheric chemistry of organic compounds and the influence of anthropogenic activities and biomass burning in remote areas. A higher time resolution (50 sample positions) combined with the measurement of boundary conditions such as solar flux and particle number would lead to in-situ observations to further refine the current knowledge. The simultaneous characterization of atmospheric particles is necessary to unambiguously relate the occurrence of several discussed VOCs to anthropogenic activities.

5 Acknowledgments

We acknowledge the financial support of the Belgian Science Policy office (BELSPO) in the framework of the CHASE (BR/175/A2/CHASE) and CLIMB (BR/175/A2/CHASE-2 and B2/191/P1/CLIMB) projects. The financial investment in analytical equipment (PTR-Qi-TOFMS) in the framework of heavy research equipment support by the Hercules foundation is acknowledged (AUGE/15/08) as well as the financial support by the special research fund (BOF) in the form of SG for Christophe Walgraeve. We would like to express our gratitude to the International Polar Foundation (IPF), in particular to Nighat “Gigi” Johnson-Amin, Alain Hubert, the field guides (Christophe, Manu, and Polo), Henri Robert, and all personnel deployed at, and in support of the Princess Elisabeth Station for the never-ending support. Finally, we thank our technical staff Lore Vandermeersch and Patrick De Wispelaere.

6 Bibliography

Aschmann, S.M., Nishino, N., Arey, J., Atkinson, R., 2011. Kinetics of the Reactions of OH Radicals with 2- and 3-Methylfuran, 2,3- and 2,5-Dimethylfuran, and E - and Z -3-Hexene-2,5-dione, and Products of OH + 2,5-Dimethylfuran. Environ. Sci. Technol. 45, 1859–1865. https://doi.org/10.1021/es103207k

Atkinson, R., 1989. Kinetics and Mechanisms of the Gas-Phase Reactions of the Hydroxyl Radical with Organic Compounds. Journal of physical and chemical reference data.

Atkinson, R., Arey, J., 2003. Atmospheric Degradation of Volatile Organic Compounds. Chem. Rev. 103, 4605–4638. https://doi.org/10.1021/cr0206420

Atkinson, R., Arey, J., 1994. Atmospheric Chemistry of Gas-Phase Polycyclic Aromatic Hydrocarbons: Formation of Atmospheric Mutagens. Environ. Health Perspect. 102, 117. https://doi.org/10.2307/3431940

Atkinson, R., Baulch, D.L., Cox, R.A., Crowley, J.N., Hampson, R.F., Hynes, R.G., Jenkin, M.E., Rossi, M.J., Troe, J., 2006. Evaluated kinetic and photochemical data for atmospheric chemistry: Volume II – gas phase reactions of organic species. Atmos. Chem. Phys. 6, 3625–4055. https://doi.org/10.5194/acp-6-3625-2006

Atkinson, R., Baulch, D.L., Cox, R.A., Crowley, J.N., Hampson, R.F., Hynes, R.G., Jenkin, M.E., Rossi, M.J., Troe, J., Wallington, T.J., 2008. Evaluated kinetic and photochemical data for atmospheric chemistry: Volume IV – gas phase reactions of organic halogen species. Atmos. Chem. Phys. 8, 4141–4496. https://doi.org/10.5194/acp-8-4141-2008

Atlas, E., UCAR/NCAR - Earth Observing Laboratory, 2009. Advanced Whole Air Sampler (AWAS) for HIAPER. https://doi.org/https://doi.org/10.5065/D65X270F

Barnes, I., Hjorth, J., Mihalapoulos, N., 2006. Dimethyl sulfide and dimethyl sulfoxide and their oxidation in the atmosphere. Chem. Rev. 106, 940–975. https://doi.org/10.1021/cr020529+

Beyersdorf, A.J., Blake, D.R., Swanson, A., Meinardi, S., Rowland, F.S., Davis, D., 2010. Abundances and variability of tropospheric volatile organic compounds at the South Pole and other Antarctic locations. Atmos. Environ. 44, 4565–4574. https://doi.org/10.1016/j.atmosenv.2010.08.025

Bierbach, A., Barnes, I., Becker, K.H., 1995. Product and kinetic study of the oh-initiated gas-phase oxidation of Furan, 2-methylfuran and furanaldehydes at ≈ 300 K. Atmos. Environ. 29, 2651–2660. https://doi.org/10.1016/1352-2310(95)00096-H

Bloss, C., Wagner, V., Jenkin, M.E., Volkamer, R., Bloss, W.J., Lee, J.D., Heard, D.E., Wirtz, K., Martin-Reviejo, M., Rea, G., Wenger, J.C., Pilling, M.J., 2005. Development of a detailed chemical mechanism (MCMv3.1) for the atmospheric oxidation of aromatic hydrocarbons. Atmos. Chem. Phys. 5, 641–664. https://doi.org/10.5194/acp-5-641-2005

Bloss, W.J., Lee, J.D., Heard, D.E., Salmon, R.A., Bauguitte, S.J.B., Roscoe, H.K., Jones, A.E., 2007. Observations of OH and HO2 radicals in coastal Antarctica. Atmos. Chem. Phys. 7, 4171–4185. https://doi.org/10.5194/acp-7-4171-2007

Boucher, O., Randall, D., Artaxo, P., Bretherton, C., Feingold, G., Forster, P., Kerminen, V.-M., Kondo, Y., Liao, H., Lohmann, U., Rasch, P., Satheesh, S.K., Sherwood, S., Stevens, B., Zhang, X.Y., 2013. Clouds and Aerosols. In: Climate Change 2013: The Physical Science Basis. Contribution of Working Group I to the Fifth Assessment Report of the Intergovernmental Panel on Climate Change, in: Stocker, T.F., D. Qin, G.-K. Plattner, M. Tignor, S.K. Allen, J. Boschung, A. Nauels, Y. Xia, V.B. and P.M.M. (Ed.), Climate Change 2013 the Physical Science Basis: Working Group I Contribution to the Fifth Assessment Report of the Intergovernmental Panel on Climate Change. Cambridge University Press, Cambridge, United Kingdom and New York, NY, USA, pp. 571–658. https://doi.org/10.1017/CBO9781107415324.016

Bourtsoukidis, E., Ernle, L., Crowley, J.N., Lelieveld, J., Paris, J.D., Pozzer, A., Walter, D., Williams, J., 2019. Non-methane hydrocarbon (C2-C8) sources and sinks around the Arabian Peninsula. Atmos. Chem. Phys. 19, 7209–7232. https://doi.org/10.5194/acp-19-7209-2019

Bruner, F., Crescenti, G., Maione, M., Mangani, F., 1994. Chlorofluorocarbons Measurement in the Lower Atmosphere of the Antarctica. Int. J. Environ. Anal. Chem. 55, 311–318. https://doi.org/10.1080/03067319408026228

Bruner, F., Maione, M., Mangani, F., 1996. New assessments on CFCs tropospheric concentration levels measured in Terra Nova Bay (Antarctica). Int. J. Environ. Anal. Chem. 62, 255–262. https://doi.org/10.1080/03067319608028138

Calvert, J.G., Atkinson, R., Becker, K.H., Kamens, R.M., Seinfeld, J.H., Wallington, T.J., Yarwood, G., 2002. The Mechanisms of Atmospheric Oxidation of the Aromatic Hydrocarbons, 1st editio. ed. Oxford University Press.

Ciccioli, P., Cecinato, A., Brancaleoni, E., Frattoni, M., Bruner, F., Maione, M., 1996a. Occurrence of Oxygenated Volatile Organic Compounds (VOC) in Antarctica. Int. J. Environ. Anal. Chem. 62, 245–253. https://doi.org/10.1080/03067319608028137

Ciccioli, P., Cecinato, A., Brancaleoni, E., Frattoni, M., Bruner, F., Maione, M., 1996b. Occurrence of Oxygenated Volatile Organic Compounds (VOC) in Antarctica. Int. J. Environ. Anal. Chem. 62, 245–253. https://doi.org/10.1080/03067319608028137

Clarkson, T.S., Martin, R.J., 1997. Ethane and Propane in the southern marine troposphere 31, 3763–3771.

Coggon, M.M., Lim, C.Y., Koss, A.R., Sekimoto, K., Yuan, B., Gilman, J.B., Hagan, D.H., Selimovic, V., Zarzana, K.J., Brown, S.S., M Roberts, J., Müller, M., Yokelson, R., Wisthaler, A., Krechmer, J.E., Jimenez, J.L., Cappa, C., Kroll, J.H., De Gouw, J., Warneke, C., 2019. OH chemistry of non-methane organic gases (NMOGs) emitted from laboratory and ambient biomass burning smoke: Evaluating the influence of furans and oxygenated aromatics on ozone and secondary NMOG formation. Atmos. Chem. Phys. 19, 14875–14899. https://doi.org/10.5194/acp-19-14875-2019

de Gouw, J., Warneke, C., 2007. Measurements of volatile organic compounds in the earth's atmosphere using proton-transfer-reaction mass spectrometry. Mass Spectrom. Rev. 26, 223–257. https://doi.org/10.1002/mas.20119

Demeestere, K., Dewulf, J., De Roo, K., De Wispelaere, P., Van Langenhove, H., 2008. Quality control in quantification of volatile organic compounds analysed by thermal desorption-gas chromatography-mass spectrometry. J Chromatogr A 1186, 348–357. https://doi.org/10.1016/j.chroma.2007.11.036

Edtbauer, A., Stönner, C., Pfannerstill, E.Y., Berasategui, M., Walter, D., Crowley, N., Lelieveld, J., Williams, J., 2020. A new marine biogenic emission : methane sulfonamide (MSAM), DMS and DMSO 2 measured in air over the Arabian Sea 1–20.

Eger, P.G., Schuladen, J., Sobanski, N., Fischer, H., Karu, E., Williams, J., Riva, M., Zha, Q., Ehn, M., Quéléver, L.L.J., Schallhart, S., Lelieveld, J., Crowley, J.N., 2020. Pyruvic acid in the boreal forest: Gas-phase mixing ratios and impact on radical chemistry. Atmos. Chem. Phys. 20, 3697–3711. https://doi.org/10.5194/acp-20-3697-2020

Fischer, R., Weller, R., Jacobi, H.-W., Ballschmiter, K., 2002. Levels and pattern of volatile organic nitrates and halocarbons in the air at Neumayer Station (70°S), Antarctic. Chemosphere 48, 981–992. https://doi.org/10.1016/s0045-6535(02)00110-8

Forster, P., Storelvmo, T., Armour, K., Collins, W., Dufresne, J.-L., Frame, D., Lunt, D.J., Mauritsen, T., Palmer, M.D., Watanabe, W., Wild, M., Zhang, H., 2021. The Earth's Energy Budget, Climate Feedbacks, and Climate Sensitivity. In Climate Change 2021: The Physical Science Basis. Contribution of Working Group I to the Sixth Assessment Report of the Intergovernmental Panel on Climate Change. Cambridge University Press, Cambridge, United Kingdom and New York, NY, USA. https://doi.org/10.1017/9781009157896.009

Franco, B., Blumenstock, T., Cho, C., Clarisse, L., Clerbaux, C., Coheur, P.F., De Mazière, M., De Smedt, I., Dorn, H.P., Emmerichs, T., Fuchs, H., Gkatzelis, G., Griffith, D.W.T., Gromov, S., Hannigan, J.W., Hase, F., Hohaus, T., Jones, N., Kerkweg, A., Kiendler-Scharr, A., Lutsch, E., Mahieu, E., Novelli, A., Ortega, I., Paton-Walsh, C., Pommier, M., Pozzer, A., Reimer, D., Rosanka, S., Sander, R., Schneider, M., Strong, K., Tillmann, R., Van Roozendael, M., Vereecken, L., Vigouroux, C., Wahner, A., Taraborrelli, D., 2021. Ubiquitous atmospheric production of organic acids mediated by cloud droplets. Nature 593, 233–237. https://doi.org/10.1038/s41586-021-03462-x

Fu, T.M., Jacob, D.J., Wittrock, F., Burrows, J.P., Vrekoussis, M., Henze, D.K., 2008. Global budgets of atmospheric glyoxal and methylglyoxal, and implications for formation of secondary organic aerosols. J. Geophys. Res. Atmos. 113. https://doi.org/10.1029/2007JD009505

Gilman, J.B., Lerner, B.M., Kuster, W.C., Goldan, P.D., Warneke, C., Veres, P.R., Roberts, J.M., De Gouw, J.A., Burling, I.R., Yokelson, R.J., 2015. Biomass burning emissions and potential air quality impacts of volatile organic compounds and other trace gases from fuels common in the US. Atmos. Chem. Phys. 15, 13915–13938. https://doi.org/10.5194/acp-15-13915-2015

Gorodetskaya, I. V., Kneifel, S., Maahn, M., Thiery, W., Schween, J.H., Mangold, A., Crewell, S., Van Lipzig, N.P.M., 2015. Cloud and precipitation properties from ground-based remote-sensing instruments in East Antarctica. Cryosphere 9, 285–304. https://doi.org/10.5194/tc-9-285-2015

Gorodetskaya, I. V., Van Lipzig, N.P.M., Van Den Broeke, M.R., Mangold, A., Boot, W., Reijmer, C.H., 2013. Meteorological regimes and accumulation patterns at Utsteinen, Dronning Maud Land, East Antarctica: Analysis of two contrasting years. J. Geophys. Res. Atmos. 118, 1700–1715. https://doi.org/10.1002/jgrd.50177

Griffiths, P.T., Murray, L.T., Zeng, G., Shin, Y.M., Abraham, N.L., Archibald, A.T., Deushi, M., Emmons, L.K., Galbally, I.E., Hassler, B., Horowitz, L.W., Keeble, J., Liu, J., Moeini, O., Naik, V., O'Connor, F.M., Oshima, N., Tarasick, D., Tilmes, S., Turnock, S.T., Wild, O., Young, P.J., Zanis, P., 2021. Tropospheric ozone in CMIP6 simulations. Atmos. Chem. Phys. 21, 4187–4218. https://doi.org/10.5194/acp-21-4187-2021

Gros, V., Martin, D., Poisson, N., Kanakidou, M., Bonsang, B., Le Guern, F., Demont, E., 1998. Ozone and C2-C5 hydrocarbon observations in the marine boundary layer between 45°S and 77°S. Tellus, Ser. B Chem. Phys. Meteorol. 50, 430–448.

https://doi.org/10.3402/tellusb.v50i5.16222

Gueneron, M., Erickson, M.H., Vanderschelden, G.S., Jobson, B.T., 2015. PTR-MS fragmentation patterns of gasoline hydrocarbons. Int. J. Mass Spectrom. 379, 97–109. https://doi.org/10.1016/j.ijms.2015.01.001

Hara, K., Osada, K., Matsunaga, K., Iwasaka, Y., Shibata, T., Furuya, K., 2002. Atmospheric inorganic chlorine and bromine species in Arctic boundary layer of the winter/spring. J. Geophys. Res. Atmos. 107, AAC 4-1-AAC 4-15. https://doi.org/10.1029/2001JD001008

Herenz, P., Wex, H., Mangold, A., Laffineur, Q., Gorodetskaya, I. V., Fleming, Z.L., Panagi, M., Stratmann, F., 2019. CCN measurements at the Princess Elisabeth Antarctica research station during three austral summers. Atmos. Chem. Phys. 19, 275–294. https://doi.org/10.5194/acp-19-275-2019

Hu, Q.H., Xie, Z.Q., Wang, X.M., Kang, H., He, Q.F., Zhang, P., 2013. Secondary organic aerosols over oceans via oxidation of isoprene and monoterpenes from Arctic to Antarctic. Sci. Rep. 3, 1–7. https://doi.org/10.1038/srep02280

Karset, I.H.H., Koren Berntsen, T., Storelvmo, T., Alterskjær, K., Grini, A., Olivié, Di., Kirkevåg, A., Seland, Ø., Iversen, T., Schulz, M., 2018. Strong impacts on aerosol indirect effects from historical oxidant changes. Atmos. Chem. Phys. 18, 7669–7690. https://doi.org/10.5194/acp-18-7669-2018

Kesselmeier, J., Kuhn, U., Wolf, A., Andreae, M.O., Ciccioli, P., Brancaleoni, E., Frattoni, M., Guenther, A., Greenberg, J., De Castro Vasconcellos, P., De Oliva, T., Tavares, T., Artaxo, P., 2000. Atmospheric volatile organic compounds (VOC) at a remote tropical forest site in central Amazonia. Atmos. Environ. 34, 4063–4072. https://doi.org/10.1016/S1352-2310(00)00186-2

Koga, S., Nomura, D., Wada, M., 2014. Variation of dimethylsulfide mixing ratio over the Southern Ocean from 36°S to 70°S. Polar Sci. 8, 306–313. https://doi.org/10.1016/j.polar.2014.04.002

Koppmann, R., 2007. Volatile Organic Compounds in the Atmosphere. Blackwell Publishing Ltd, Oxford, UK. https://doi.org/10.1002/9780470988657

Koss, A.R., Sekimoto, K., Gilman, J.B., Selimovic, V., Coggon, M.M., Zarzana, K.J., Yuan, B., Lerner, B.M., Brown, S.S., Jimenez, J.L., Krechmer, J., Roberts, J.M., Warneke, C., Yokelson, R.J., De Gouw, J., 2018. Non-methane organic gas emissions from biomass burning: Identification, quantification, and emission factors from PTR-ToF during the FIREX 2016 laboratory experiment. Atmos. Chem. Phys. 18, 3299–3319. https://doi.org/10.5194/acp-18-3299-2018

Kroupa, A., Dewulf, J., Van Langenhove, H., Víden, I., 2004. Breakthrough characteristics of volatile organic compounds in the -10 to +170°C temperature range on Tenax TA determined by microtrap technology. J. Chromatogr. A 1038, 215–223. https://doi.org/10.1016/j.chroma.2004.03.035

Kuo, T.-C., Tan, C.-E., Wang, S.-Y., Lin, O.A., Su, B.-H., Hsu, M.-T., Lin, J., Cheng, Y.-Y., Chen, C.-S., Yang, Y.-C., Chen, K.-H., Lin, S.-W., Ho, C.-C., Kuo, C.-H., Tseng, Y.J., 2020. Human Breathomics Database. Database 2020. https://doi.org/10.1093/database/baz139

Kwok, E., Atkinson, R., 1995. Estimation of hydroxyl radical reaction rate constants for gas-phase organic compounds using a structure-reactivity relationship: An update. Atmos. Environ. 29, 1685–1695. https://doi.org/10.1016/1352-2310(95)00069-B

Lerner, B.M., Gilman, J.B., Aikin, K.C., Atlas, E.L., Goldan, P.D., Graus, M., Hendershot, R., Isaacman-Vanwertz, G.A., Koss, A., Kuster, W.C., Lueb, R.A., Mclaughlin, R.J., Peischl, J., Sueper, D., Ryerson, T.B., Tokarek, T.W., Warneke, C., Yuan, B., De Gouw, J.A., 2017. An improved, automated whole air sampler and gas chromatography mass spectrometry analysis system for volatile organic compounds in the atmosphere. Atmos. Meas. Tech. 10, 291–313. https://doi.org/10.5194/amt-10-291-2017

Lindinger, W., Hansel, A., Jordan, A., 1998. On-line monitoring of volatile organic compounds at pptv levels by means of Proton-Transfer-Reaction Mass Spectrometry (PTR-MS) Medical applications, food control and environmental research. Int. J. Mass Spectrom. Ion Process. 173, 191–241. https://doi.org/10.1016/s0168-1176(97)00281-4

Lopez-Hilfiker, F., Zhu, L., Hutterli, M., Cappellin, L., 2019. Calibrating Vocus PTR-TOF Sensitivity Using a Subset of VOC Standards 1–4.

Magi, E., Tanwar, S., 2014. “Extreme mass spectrometry”: the role of mass spectrometry in the study of the Antarctic environment. J Mass Spectrom 49, 1071–1085. https://doi.org/10.1002/jms.3442

Markes international, 2014. SafeLok FAQs.

Mellouki, A., Wallington, T.J., Chen, J., 2015. Atmospheric Chemistry of Oxygenated Volatile Organic Compounds: Impacts on Air Quality and Climate. Chem. Rev. 115, 3984–4014. https://doi.org/10.1021/cr500549n

Olariu, R.I., Barnes, I., Becker, K.H., Klotz, B., 2000. Rate coefficients for the gas-phase reaction of OH radicals with selected dihydroxybenzenes and benzoquinones. Int. J. Chem. Kinet. 32, 696–702. https://doi.org/10.1002/1097-4601(2000)32:11<696::AID-KIN5>3.0.CO;2-N

Pattyn, F., Matsuoka, K., Berte, J., 2009. Glacio-meteorological conditions in the vicinity of the Belgian Princess Elisabeth Station, Antarctica. Antarct. Sci. 22, 79–85. https://doi.org/10.1017/S0954102009990344

Pleil, J.D., Hansel, A., Beauchamp, J., 2019. Advances in proton transfer reaction mass spectrometry (PTR-MS): Applications in exhaled breath analysis, food science, and atmospheric chemistry. J. Breath Res. 13. https://doi.org/10.1088/1752-7163/ab21a7

Preunkert, S., Jourdain, B., Legrand, M., Udisti, R., Becagli, S., Cerri, O., 2008. Seasonality of sulfur species (dimethyl sulfide, sulfate, and methanesulfonate) in Antarctica: Inland versus coastal regions. J. Geophys. Res. Atmos. 113. https://doi.org/10.1029/2008JD009937

Preunkert, S., Legrand, M., Jourdin, B., Moulin, C., Belviso, S., Kasamatsu, N., Fukuchi, M., Hirawake, T., 2007. Interannual variability of dimethylsulfide in air and seawater and its atmospheric oxidation by-products (methanesulfonate and sulfate) at Dumont d'Urville, coastal Antarctica (1999-2003). J. Geophys. Res. Atmos. 112, 1–13. https://doi.org/10.1029/2006JD007585

Quack, B., Wallace, D.W.R., 2003. Air-sea flux of bromoform: Controls, rates, and implications. Global Biogeochem. Cycles 17. https://doi.org/10.1029/2002GB001890

Rasmussen, R. a., Khalil, M. a. K., 1999. Atmospheric methyl chloride. Atmos. Environ. 33, 1305–1321.

Read, K.A., Lewis, A.C., Bauguitte, S., Rankin, A.M., Salmon, R.A., Wolff, E.W., Saiz-Lopez, A., Bloss, W.J., Heard, D.E., Lee, J.D., Plane, J.M.C., 2008. DMS and MSA measurements in the Antarctic Boundary Layer: Impact of BrO on MSA production. Atmos. Chem. Phys. 8, 2985–2997. https://doi.org/10.5194/acp-8-2985-2008

Read, K.A., Lewis, A.C., Salmon, R.A., Jones, A.E., Bauguitte, S., 2007. OH and halogen atom influence on the variability of non-methane hydrocarbons in the Antarctic Boundary Layer. Tellus, Ser. B Chem. Phys. Meteorol. 59, 22–38. https://doi.org/10.1111/j.1600-0889.2006.00226.x

Roquencourt, C., 2021. ptairMS: Pre-processing PTR-TOF-MS Data. R package version 1.2.0.

Roquencourt, C., Grassin-Delyle, S., Thévenot, E.A., 2022. ptairMS: real-time processing and analysis of PTR-TOF-MS data for biomarker discovery in exhaled breath. Bioinformatics 1–8. https://doi.org/10.1093/bioinformatics/btac031

Rossabi, S., Helmig, D., 2018. Changes in Atmospheric Butanes and Pentanes and Their Isomeric Ratios in the Continental United States. J. Geophys. Res. Atmos. 123, 3772–3790. https://doi.org/10.1002/2017JD027709

Rudolph, J., Khedim, A., Clarkson, T., Wagenbach, D., 1992a. Long-term measurements of light alkanes and acetylene in the Antarctic troposphere. Tellus B Chem. Phys. Meteorol. 44, 252–261. https://doi.org/10.3402/tellusb.v44i4.15453

Rudolph, J., Khedim, A., Clarkson, T., Wagenbach, D., Khedim, A., Clarkson, T., Long-term, D.W., 1992b. Chemical and Physical Meteorology Long-term measurements of light alkanes and acetylene in the Antarctic troposphere Long-term measurements of light alkanes and acetylene in the Antarctic troposphere 0889. https://doi.org/10.3402/tellusb.v44i4.15453

Rudolph, J., Khedim, A., Wagenbach, D., 1989. The seasonal variation of light nonmethane hydrocarbons in the Antarctic troposphere. J. Geophys. Res. Atmos. 94, 13039–13044. https://doi.org/10.1029/JD094iD10p13039

Salta, Z., Kosmas, A.M., Segovia, M.E., Kieninger, M., Tasinato, N., Barone, V., Ventura, O.N., 2020. Reinvestigation of the Deceptively Simple Reaction of Toluene with OH and the Fate of the Benzyl Radical: The "hidden" Routes to Cresols and Benzaldehyde. J. Phys. Chem. A 124, 5917–5930. https://doi.org/10.1021/acs.jpca.0c03727

Schwarz, K., Filipiak, W., Amann, A., 2009. Determining concentration patterns of volatile compounds in exhaled breath by PTR-MS. J. Breath Res. 3. https://doi.org/10.1088/1752-7155/3/2/027002

Selimovic, V., Ketcherside, D., Chaliyakunnel, S., Wielgasz, C., Permar, W., Angot, H., Millet, D.B., Fried, A., Helmig, D., Hu, L., 2022. Atmospheric biogenic volatile organic compounds in the Alaskan Arctic tundra: constraints from measurements at Toolik Field Station. Atmos. Chem. Phys. 22, 14037–14058. https://doi.org/10.5194/acp-22-14037-2022

Shrivastava, M., Cappa, C.D., Fan, J., Goldstein, A.H., Guenther, A.B., Jimenez, J.L., Kuang, C., Laskin, A., Martin, S.T., Ng, N.L., Petaja, T., Pierce, J.R., Rasch, P.J., Roldin, P., Seinfeld, J.H., Shilling, J., Smith, J.N., Thornton, J.A., Volkamer, R., Wang, J., Worsnop, D.R., Zaveri, R.A., Zelenyuk, A., Zhang, Q., 2017. Recent advances in understanding secondary organic aerosol: Implications for global climate forcing. Rev. Geophys. 55, 509–559. https://doi.org/10.1002/2016RG000540

Simon, V., Riba, M.L., Fugit, J.L., Dutaur, L., Torres, L., 1996. Study of isoprene and α-pinene breakthrough volume on Tenax

TA. Chem. Analityczna 41, 233–240.

Simon, V., Riba, M.L., Waldhart, A., Torres, L., 1995. Breakthrough volume of monoterpenes on Tenax TA: influence of temperature and concentration for α-pinene. J. Chromatogr. A 704, 465–471. https://doi.org/10.1016/0021-9673(95)00213-7

Slusher, D.L., Neff, W.D., Kim, S., Huey, L.G., Wang, Y., Zeng, T., Tanner, D.J., Blake, D.R., Beyersdorf, A., Lefer, B.L., Crawford, J.H., Eisele, F.L., Mauldin, R.L., Kosciuch, E., Buhr, M.P., Wallace, H.W., Davis, D.D., 2010. Atmospheric chemistry results from the ANTCI 2005 Antarctic plateau airborne study. J. Geophys. Res. Atmos. 115, 1–18. https://doi.org/10.1029/2009JD012605

Stockwell, C.E., Veres, P.R., Williams, J., Yokelson, R.J., 2015. Characterization of biomass burning emissions from cooking fires, peat, crop residue, and other fuels with high-resolution proton-transfer-reaction time-of-flight mass spectrometry. Atmos. Chem. Phys. 15, 845–865. https://doi.org/10.5194/acp-15-845-2015

Swanson, A.L., Davis, D.D., Arimoto, R., Roberts, P., Atlas, E.L., Flocke, F., Meinardi, S., Sherwood Rowland, F., Blake, D.R., 2004. Organic trace gases of oceanic origin observed at South Pole during ISCAT 2000. Atmos. Environ. 38, 5463–5472. https://doi.org/10.1016/j.atmosenv.2004.03.072

Tosato, M.L., Chiorboli, C., Eriksson, L., Jonsson, J., 1991. Multivariate modelling of the rate constant of the gas-phase reaction of haloalkanes with the hydroxyl radical. Sci. Total Environ. 109–110, 307–325. https://doi.org/10.1016/0048-9697(91)90187-J

Verreyken, B., Amelynck, C., Brioude, J., Muller, J.F., Schoon, N., Kumps, N., Colomb, A., Metzger, J.M., Lee, C.F., Koenig, T.K., Volkamer, R., Stavrakou, T., 2020. Characterisation of African biomass burning plumes and impacts on the atmospheric composition over the south-west Indian Ocean. Atmos. Chem. Phys. 20, 14821–14845. https://doi.org/10.5194/acp-20-14821-2020

Villanueva, F., Cabañas, B., Monedero, E., Salgado, S., Bejan, I., Martin, P., 2009. Atmospheric degradation of alkylfurans with chlorine atoms: Product and mechanistic study. Atmos. Environ. 43, 2804–2813. https://doi.org/10.1016/j.atmosenv.2009.02.030

Warneck, P., 2005. Multi-Phase Chemistry of C2 and C3 organic compounds in the marine atmosphere. J. Atmos. Chem. 51, 119–159. https://doi.org/10.1007/s10874-005-5984-7

Wevill, D.J., Carpenter, L.J., 2004. Automated measurement and calibration of reactive volatile halogenated organic compounds in the atmosphere. Analyst 129, 634–638. https://doi.org/10.1039/b403550j

Woolfenden, E., 2012. Thermal Desorption for Gas Chromatography, Gas Chromatography. https://doi.org/10.1016/B978-0-12-385540-4.00010-9

Woolfenden, E., Cole, A., 2003. Sampling Device - US 6564656 B1. 6564656.

Xu, X., Williams, J., Plass-Dülmer, C., Berresheim, H., Salisbury, G., Lange, L., Lelieveld, J., 2003. GC×GC measurements of C7-C11 aromatic and n-alkane hydrocarbons on Crete, in air from Eastern Europe during the MINOS campaign. Atmos. Chem. Phys. 3, 1461–1475. https://doi.org/10.5194/acp-3-1461-2003

Yuan, B., Koss, A.R., Warneke, C., Coggon, M., Sekimoto, K., De Gouw, J.A., 2017. Proton-Transfer-Reaction Mass Spectrometry: Applications in Atmospheric Sciences. Chem. Rev. 117, 13187–13229. https://doi.org/10.1021/acs.chemrev.7b00325

Yuan, Y., Zhao, X., Wang, S., Wang, L., 2017. Atmospheric Oxidation of Furan and Methyl-Substituted Furans Initiated by Hydroxyl Radicals. J. Phys. Chem. A 121, 9306–9319. https://doi.org/10.1021/acs.jpca.7b09741

Zemmelink, H.J., Gieskes, W.W.C., Holland, P.M., Dacey, J.W.H., 2002. Preservation of atmospheric dimethyl sulphide samples on Tenax in sea-to-air flux measurements. Atmos. Environ. 36, 911–916. https://doi.org/10.1016/S1352-2310(01)00535-0

Zenkevich, I.G., 2005. Experimentally measured retention indices.

Zoccolillo, L., Amendola, L., Insogna, S., 2009. Comparison of atmosphere/aquatic environment concentration ratio of volatile chlorinated hydrocarbons between temperate regions and Antarctica. Chemosphere 76, 1525–1532. https://doi.org/10.1016/j.chemosphere.2009.05.044

Zoccolillo, L., Amendola, L., Insogna, S., Pastorini, E., 2010. On-line analysis of volatile chlorinated hydrocarbons in air by gas chromatography-mass spectrometry Improvements in preconcentration and injection steps. J Chromatogr A 1217, 3890–3895. https://doi.org/10.1016/j.chroma.2010.04.013

Supplementary Information

S.I. 1: Concentrations of the compounds in the external standards used together with the relative sample response factor (RSRF) found by the calibration procedure.

Compound	CAS	Concentration (ng/µL)	RSRF TD-GC-MS	RSRF TD-PTR-Qi-TOFMS
Standard A				
n-Pentane	109-66-0	31.3	0.13	
n-Hexane	110-54-3	32.95	0.12	
1,1,2-trichloro-1,2,2-trifluoroethane	76-13-1	78.5	0.02	
Trichloromethane	67-66-3	74.6	0.26	
1,2-dichloroethane	107-06-2	62.65	0.15	
Carbon Tetrachloride	56-23-5	79.7	0.25	
n-Butanal	123-72-8	40.85	0.10	1.39
Benzene	71-43-2	43.7	0.18	2.24
Toluene	108-88-3	43.3	1.00	0.99
Ethylbenzene	100-41-4	43.35	0.90	
Styrene	100-42-5	45.45	0.81	1.01
Acetophenone	98-86-2	51.5	1.16	0.66
Standard B				
Dimethylsulfide	75-18-3	42		1.168
Furan	110-00-9	46.8	0.13	0.73
2-butanone	78-93-3	40.3	0.27	1.90
m-xylene	108-38-3	43.4	1.16	1.32
Benzaldehyde	100-52-7	52.5	0.57	0.89
Benzonitril	100-47-0	50.5	0.99	2.01
Phenol	108-95-2	48.8	0.53	0.80
Standard C				
Trichloromonofluoromethane	75-69-4	74.5	0.10	
Tribromomethane	75-25-2	144.5	0.33	
Dimethylsulfone	67-71-0	32.5	0.07	1.24
Phenylacetylene	536-74-3	46.5	0.87	1.62
p-Benzoquinone	106-51-4	27.5	0.03	0.83
Phenylacetaldehyde	122-78-1	54	0.13	0.26
Methylbenzoate	93-58-3	54.5	1.52	0.94
Benzophenone	119-61-9	33	0.70	0.79
Standard D				
2-hydroxyacetophenone	118-93-4	56.5	0.70	0.84
Phenylacetic acid	103-82-2	31	0.68	0.84
Benzoylformic acid	611-73-4	69	0.68	0.58
Phtalic acid	88-99-3	31.5	0.17	
Standard E				
2-furaldehyde	498-60-2	57.5	0.31	1.22
3-hydroxybenzaldehyde	100-83-4	41.5	0.05	0.89
Benzofuran	271-89-6	53.6	0.82	1.24
Benzoic acid phenyl ester	93-99-2	30	0.61	0.26
1,2-diphenyl Ethanone	451-40-1	27.5	0.25	1

S.I. 2: Flow measured with the internal (Honeywell HAF 200 sccm) flowmeter inserted in the flow path between the sorbent tube and the pump. A 1000 ms sample frequency was used. Flow at t=0 and t=3600 min with a TSI flowmeter connected to the sorbent tube inlet.

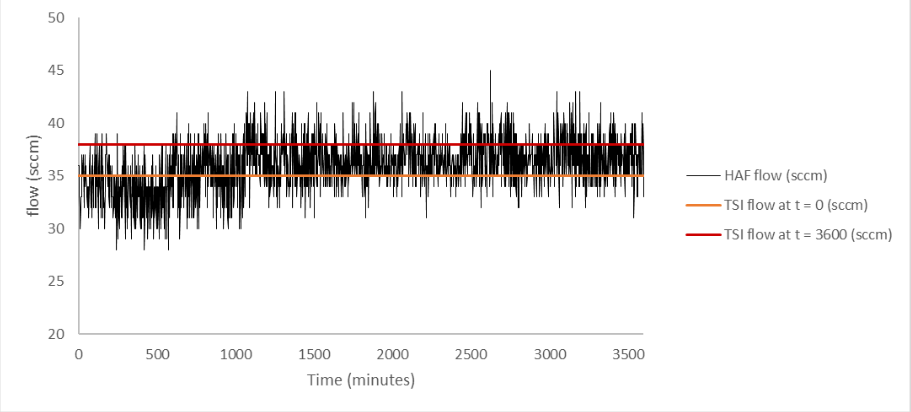

S.I. 3: Graphic representation of the sample analyse procedure. The sampled tube is desorbed and trapped in a microtrap during step 1 after which the split flow added during the microtrap desorption is recollected on a conditioned sorbent tube. During step 2 the recollection tube is desorbed in the TD-PTR-Qi-TOFMS instrument.

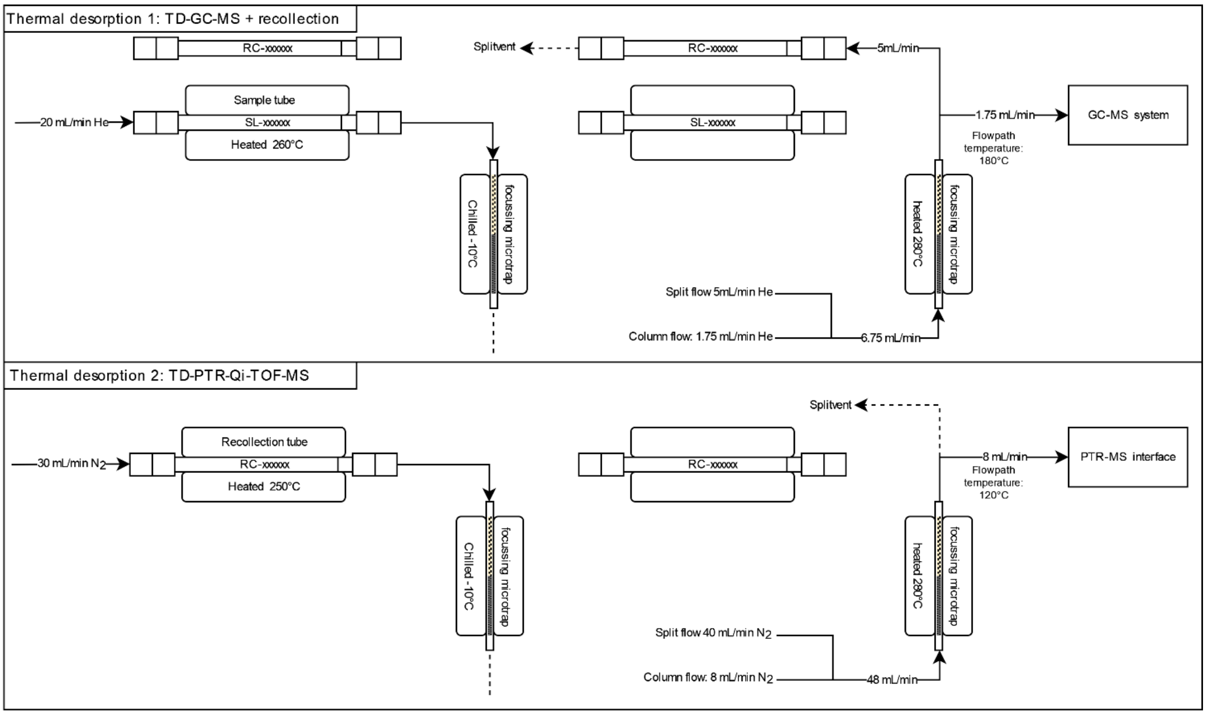

S.I. 4: The response of 10.8 ng toluene-d8 loaded on sorbent tubes was tested to verify the linearity, in function of the split factor, determined by the trap desorption split flow, of this novel instrumental combination. Each point was measured in triplicate except for split = 0 (n=2).

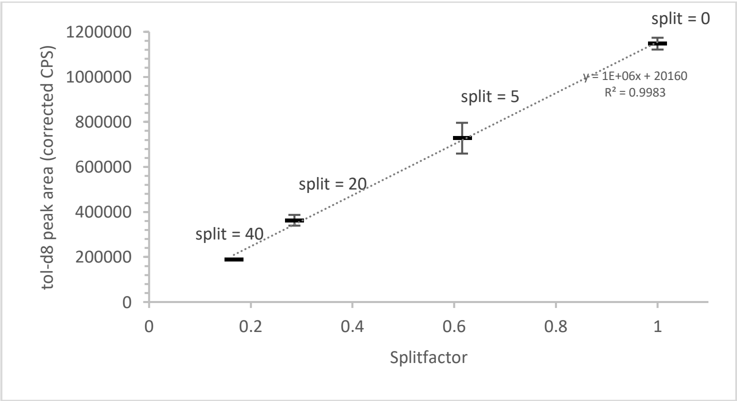

S.I. 5: Decision tree used to categorize the found compounds according to the amount of breakthrough determined from the described field experiment, or from theory.

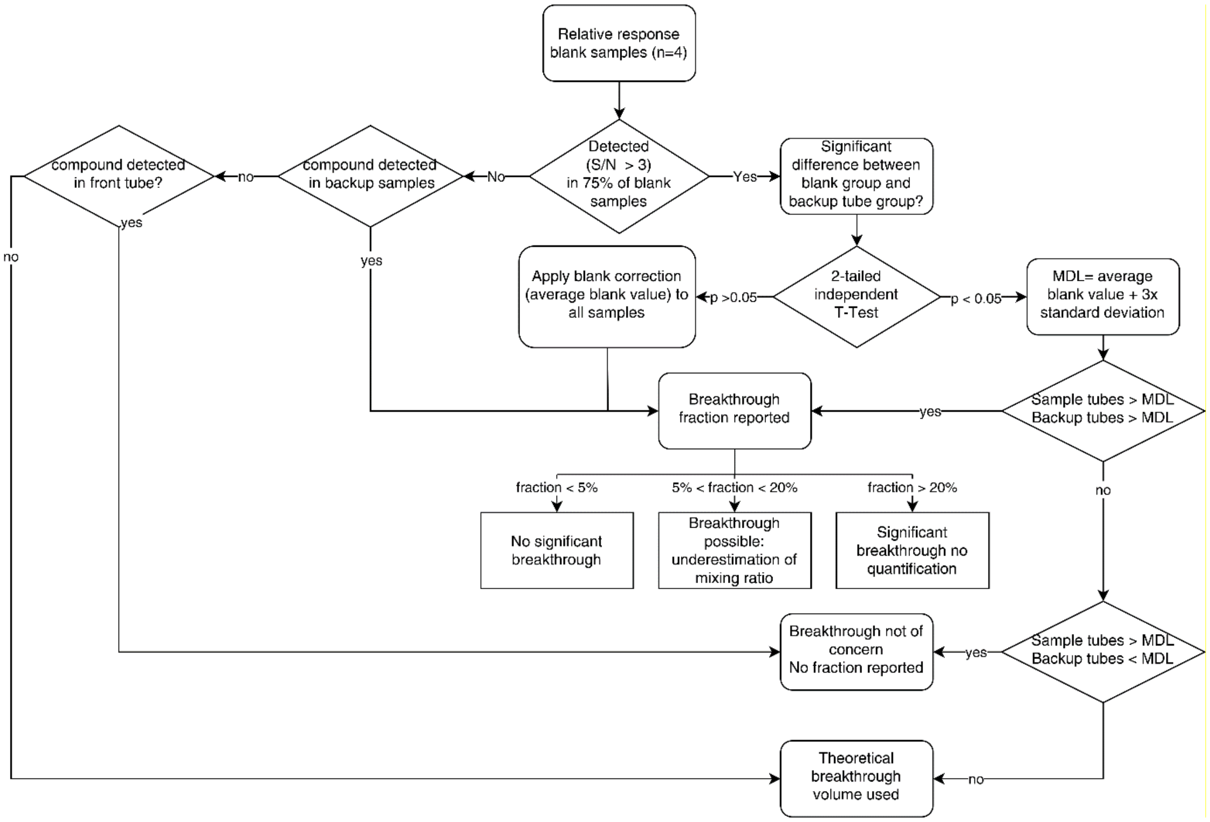

S.I. 6: Results of the breakthrough experiment conducted during the 2019-2020 sampling campaign. N.D.; the compound was not detected in the backup tube, <MDL; the compound was detected in the backup tube but remained under the method detection limit. "-" indicates the compound was not detected in the front tube. * recalculated data from www.sisweb.com/index/referenc/tenaxta.htm (last accessed 01/11/2022)

Compound	Mass ratio (%) (RPA$_{backup}$/RPA$_{front}$) x 100	RSD (n=6) (%)	BTV (theoretical at 0°C) (L/200mg)*	Category
Glyoxal	0.7	1	Not reported	No significant breakthrough
Trichlorofluoromethane	116.4	25	2	Significant breakthrough
Furan	<MDL	-	Not reported	No significant breakthrough
Methylene chloride	109.8	12	4	Significant breakthrough
Trichlorotrifluoroethane	133.9	35	Not reported	Significant breakthrough
Formic acid	<MDL	-	Not reported	No significant breakthrough
Butanal	73.4	49	38	Significant breakthrough
2-butanone	56.5	42	50	Significant breakthrough
Acetic acid	<MDL	-	6	No significant breakthrough
Trichloromethane	86.8	20	20	Significant breakthrough
1,2-dichloroethane	30.4	12	32	Significant breakthrough
1,1,1-trichloroethane	91.7	21	10	Significant breakthrough
Benzene	2.6	2	82	No significant breakthrough
Carbon tetrachloride	94.1	20	24	Significant breakthrough
Toluene	10.6	12	1620	Breakthrough possible
Methanesulfonyl chloride	0.2	0	Not reported	No significant breakthrough
Hexanal	55.7	9	800	Significant breakthrough
Butyric acid	N.D.	-	200	No significant breakthrough
2-furaldehyde	N.D.	-	Not reported	No significant breakthrough
Ethylbenzene	<MDL	-	2500	No significant breakthrough
m-xylene	<MDL	-	2700	No significant breakthrough
Phenylethyne	4.9	1	Not reported	No significant breakthrough
Tribromomethane	N.D.	-	1600	No significant breakthrough
Dimethylsulfone	N.D.	-	Not reported	No significant breakthrough
Styrene	-	-	2700	No significant breakthrough
p-Benzoquinone	N.D.	-	Not reported	No significant breakthrough
o-xylene	-	-	2900	No significant breakthrough
Benzaldehyde	<MDL	-	1580	No significant breakthrough
Ethoxy-benzene	N.D.	-	Not reported	No significant breakthrough
Benzonitril	7.5	4	Not reported	Breakthrough possible
Phenol	<MDL	-	8000	No significant breakthrough
Octanal	-	-	31600	No significant breakthrough
Phenylacetaldehyde	<MDL	-	Not reported	No significant breakthrough
3-hydroxy benzaldehyde	<MDL	-	Not reported	No significant breakthrough
Propoxybenzene	N.D.	-	Not reported	No significant breakthrough
Acetophenone	<MDL	-	Not reported	No significant breakthrough
Phenylglyoxal	N.D.	-	Not reported	No significant breakthrough
Methyl benzoate	N.D.	-	Not reported	No significant breakthrough
1,3-Benzodioxol-2-one	N.D.	-	Not reported	No significant breakthrough
Benzoic acid	<MDL	-	Not reported	No significant breakthrough
2-Coumaranone	2.8	3	Not reported	No significant breakthrough
2-hydroxy-1-phenyl	N.D.	-	Not reported	No significant breakthrough
Benzeneacetic acid	<MDL	-	Not reported	No significant breakthrough
Benzoylformic acid	N.D.	-	Not reported	No significant breakthrough
2,3-Benzofurandione	<MDL	-	Not reported	No significant breakthrough
Phtalic acid	<MDL	-	Not reported	No significant breakthrough
2-ethoxy benzaldehyde	N.D.	-	Not reported	No significant breakthrough
Phenylmaleic anhydride	<MDL	-	Not reported	No significant breakthrough
Benzophenone	1.8	3	Not reported	No significant breakthrough
Phenyl benzoate	N.D.	-	Not reported	No significant breakthrough
1,2-diphenyl ethanone	<MDL	-	Not reported	No significant breakthrough

S.I. 7: MDL and MQL values (in µg) for all reported compounds for both TD-GC-MS and TD-PTR-Qi-TOFMS. The reader is advised that the reported MDL and MQL values are mainly the effect of the diffusion through the SAFELOK insert and in no way reflect the actual instrumental detection limits.

Compound		TD-GC-MS		TD-PTR-Qi-TOFMS	
	CAS	MDL (µg)	MQL (µg)	MDL (µg)	MQL (µg)
n-Pentane	109-66-0	0.0025	0.0049		
n-Hexane	110-54-3	0.0112	0.0235		
Isoprene	78-79-5			0.0217	0.0440
Trichloromonofluoromethane (Freon 11)	75-69-4	0.0868	0.1313		
1,1,2-trichloro-1,2,2-trifluoroethane (Freon 113)	76-13-1	0.6157	1.0413		
Methylene chloride (Freon-30)	75-09-2	0.0019	0.0022		
Trichloromethane (Freon 20)	67-66-3	0.0065	0.0095		
1,2-dichloroethane (Freon 150)	107-06-2	0.0017	0.0023		
1,1,1-trichloroethane (Freon 140a)	71-55-6	0.0035	0.0051		
Carbon Tetrachloride (Freon-10)	56-23-5	0.1745	0.2656		
Tribromomethane	75-25-2	0.0015	0.0019		
Bromomethane	74-96-4	0.0003	0.0005		
Dimethylsulfide	75-18-3			0.0008	0.0014
Methanesulfonic anhydride	7143-03-3	0.0522	0.0774		
Methanesulfonyl Chloride	124-63-0	0.0073	0.0158	0.0014	0.0031
Dimethylsulfone	67-71-0	0.0187	0.0312	0.0121	0.0193
Glyoxal	107-22-2	0.0017	0.0043		
Furan	110-00-9	0.0054	0.0097	0.0047	0.0073
Formic acid	64-18-6	0.0984	0.2295	0.0244	0.0451
n-Butanal	123-72-8	0.0035	0.0053	0.0088	0.0130
2-butanone	78-93-3	0.0070	0.0105	0.0088	0.0130
Acetic Acid	64-19-7	0.1512	0.3133	0.2061	0.3970
Hexanal	66-25-1	0.0122	0.0291		
Butyric Acid	107-92-6	0.0069	0.0117	0.0100	0.0136
2-Furaldehyde	498-60-2	0.0011	0.0020	0.0050	0.0073
Octanal	124-13-0	0.0247	0.0607	0.0019	0.0034
Acroleine	107-02-8				
Methacrolein	78-85-3			0.0051	0.0067
Methylglyoxal	78-98-8			0.0057	0.0072
Propanoic Acid	79-09-4			0.0278	0.0557
2-Methylfuran	534-22-5			0.0021	0.0028
Butenedial	2363-83-9			0.0031	0.0042
Biacetyl	431-03-8			0.0104	0.0234
Pentanal	110-62-3			0.0034	0.0047
2-Pentanone	107-87-9			0.0034	0.0047
Pyruvic acid	127-17-3			0.0009	0.0013
Maleic Anhydride	108-31-6			0.0063	0.0108
Benzene	71-43-2	0.0085	0.0128	0.0704	0.1545
Toluene	108-88-3	0.0019	0.0027	0.0043	0.0063
Ethylbenzene	100-41-4	0.0002	0.0003		
m-xylene	108-38-3	0.0002	0.0002	0.0559	0.1155
Phenylacetylene	536-74-3	0.0014	0.0032	0.0066	0.0124
Styrene	100-42-5	0.0005	0.0009		
p-Benzoquinone	106-51-4	0.0070	0.0078	0.0062	0.0110
o-xylene	95-47-6	0.0001	0.0002	0.0559	0.1155
Benzaldehyde	100-52-7	0.1133	0.1517	0.2150	0.3054
Benzonitril	100-47-0	0.0007	0.0011	0.0016	0.0020
Phenol	108-95-2	0.0463	0.0541	0.1134	0.2311
Benzofuran	271-89-6			0.0005	0.0008
Phenylacetaldehyde	122-78-1	0.2027	0.4531	0.0005	0.0008
3-hydroxybenzaldehyde	100-83-4	0.0715	0.1506	0.2096	0.5331
Propoxybenzene	622-85-5	0.0003	0.0006		
Acetophenone	98-86-2	0.0919	0.2004	0.0005	0.0008
Phenylglyoxal	1074-12-0	0.0515	0.1258	0.0333	0.0759
Methylbenzoate	93-58-3	0.0002	0.0002	0.0033	0.0067
1,3-Benzodioxol-2-one	2171-74-6	0.0010	0.0022	0.0030	0.0062
Benzoic acid	65-85-0	0.5381	0.8470	0.2096	0.5331
2-Coumaranone	553-86-6	0.0061	0.0137	0.0333	0.0759
2-hydroxyacetophenone	118-93-4	0.0008	0.0018	0.0033	0.0067
Phenylacetic acid	103-82-2	0.0065	0.0159	0.0033	0.0067
Benzoylformic acid	611-73-4	0.0006	0.0013	0.0014	0.0023
2,3-Benzofurandione	4732-72-3	0.0196	0.0355	0.0312	0.0584
Phtalic acid	88-99-3	0.1022	0.2149	0.0023	0.0043
2-ethoxybenzaldehyde	613-69-4	0.0004	0.0009		
Phenylmaleic anhydride	36122-35-7	0.2160	0.5038	0.0435	0.1177
Benzophenone	119-61-9	0.0083	0.0189	0.0047	0.0066
Benzoic acid phenyl ester	93-99-2	0.0028	0.0065	0.0013	0.0020
1,2-diphenyl Ethanone	451-40-1	0.0249	0.0564	0.0001	0.0004

S.I. 8: Theoretical and experimental 2nd order reaction rates of the studied VOCs. The theoretical values are obtained from the EPA EPIsuite (V4.11) AOPWIN model. For the theoretical lifetime an •OH concentration of 3.10^5 molecules.cm^{-3} (Bloss et al., 2007) and 24h sunlight per day is used.

	Theoretical K_{OH} (10^{-12} cm^3 molecule^{-1} sec^{-1})	Theoretical lifetime in days (τ) assuming 3.10^5 OH.cm^{-1}	Experimental K_{OH} (10^{-12} cm^3 molecule^{-1} sec^{-1})	
n-Pentane	4.05	9.5	3.8	(Atkinson and Arey, 2003)
n-Hexane	5.46	7.1	5.2	(Atkinson and Arey, 2003)
Isoprene	105.14	0.4	100	(Atkinson et al., 2006)
Trichloromonofluoromethane (Freon 11)	0.00	-	<0.000005	(Atkinson et al., 2008)
1,1,2-trichloro-1,2,2-trifluoroethane (Freon 113)	0.00	-		
Methylene chloride (Freon-30)	0.13	286	0.1	(Atkinson et al., 2008)
Trichloromethane (Freon 20)	0.11	362	0.105	(Atkinson et al., 2008)
1,2-dichloroethane (Freon 150)	0.26	151	0.248	(Kwok and Atkinson, 1995)
1,1,1-trichloroethane (Freon 140a)	0.01	4104	0.0095	(Atkinson et al., 2008)
Carbon Tetrachloride (Freon-10)	0.00	-	<0.0005	(Atkinson et al., 2008)
Tribromomethane	0.04	906	0.148	(Atkinson et al., 2008)
Bromomethane	0.32	119	0.35	(Tosato et al., 1991)
Dimethylsulfide	3.82	10.1	4.82	(Atkinson and Arey, 1994)
Methanesulfonyl Chloride	1.06	36.4		
Dimethylsulfone	2.12	18.2		
Glyoxal	25.32	1.5	11	(Atkinson et al., 2006)
Furan	40.50	1.0	40.5	(Atkinson, 1989)
Formic acid	0.52	74.2	0.45	(Atkinson et al., 2006)
n-Butanal	25.43	1.5	24	(Atkinson et al., 2006)
2-butanone	1.33	28.9	1.2	(Atkinson et al., 2006)
Acetic Acid	0.62	62.0	0.74	(Atkinson et al., 2006)
Hexanal	28.83	1.3	30	(Atkinson and Arey, 2003)
Butyric Acid	2.70	14.3	2.4	(Atkinson, 1989)
2-Furaldehyde	37.42	1.0	48.5	(Bierbach et al., 1995)
Octanal	31.66	1.2		
Acroleine	25.82	1.5	19.9	(Atkinson, 1989)
Methacrolein	34.49	1.1	29	(Atkinson et al., 2006)
Methylglyoxal	12.76	3.0	15	(Atkinson et al., 2006)
Propanoic Acid	1.39	27.8	1.2	(Atkinson et al., 2006)
2-Methylfuran	105.87	0.4	73.1	(Aschmann et al., 2011)
Butenedial	40.28	1.0	24.1	(Bierbach et al., 1995)
Biacetyl	0.20	189	0.238	(Atkinson, 1989)
Pentanal	27.42	1.4	28	(Atkinson and Arey, 2003)
2-Pentanone	4.77	8.1	4.4	(Atkinson and Arey, 2003)
Pyruvic acid	0.62	62.0		
Maleic Anhydride	2.26	17.1	1.45	(Bierbach et al., 1995)
Benzene	1.95	19.8	1.22	(Atkinson and Arey, 2003)
Toluene	5.23	7.4	5.93	(Atkinson and Arey, 2003)
Ethylbenzene	5.95	6.5	7	(Atkinson and Arey, 2003)
m-xylene	13.56	2.8	23.1	(Atkinson and Arey, 2003)
Phenylacetylene	8.02	4.8		
Styrene	28.13	1.4	58	(Atkinson and Arey, 2003)
p-Benzoquinone	4.51	8.6	4.6	(Olariu et al., 2000)
o-xylene	6.51	5.9	13.6	(Atkinson and Arey, 2003)
Benzaldehyde	17.87	2.2	12	(Atkinson and Arey, 2003)
Benzonitril	0.34	112	0.33	(Atkinson, 1989)
Phenol	33.47	1.2	26.3	(Atkinson, 1989)
Benzofuran	37.30	1.0	37.3	(Atkinson, 1989)
Phenylacetaldehyde	26.31	1.5		
3-hydroxybenzaldehyde	33.92	1.1		
Propoxybenzene	31.95	1.2		
Acetophenone	1.88	20.5	2.74	(Atkinson, 1989)
Phenylglyoxal	14.44	2.7		
Methylbenzoate	0.84	45.7		
1,3-Benzodioxol-2-one	1.48	26.1		
Benzoic acid	1.24	31.1		
2-Coumaranone	2.56	15.1		
2-hydroxyacetophenone	30.62	1.3		
Phenylacetic acid	4.45	8.7		
Benzoylformic acid	2.30	16.8		
2,3-Benzofurandione	1.83	21.0		
Phtalic acid	1.24	31.2		
2-ethoxybenzaldehyde	30.13	1.3		
Phenylmaleic anhydride	12.48	3.1		
Benzophenone	3.55	10.9		
Benzoic acid phenyl ester	3.79	10.2		
1,2-diphenyl Ethanone	7.32	5.3		

S.I. 9: Autosampler metadata recorded during the 2019-2020 sampling campaign. Sample volume derived from the internal flow sensor. * indicates no sample was taken at the planned time.

Position	Sample Volume (L)	Start	Stop
1	215	12/12/2019 19:36	15/12/2019 19:46
2	130	19/12/2019 12:15	22/12/2019 12:36
3	222	1/1/2020 12:28	4/1/2020 12:38
4	228	14/1/2020 12:29	17/1/2020 12:39
5	220	27/1/2020 12:31	30/1/2020 12:41
6	218	9/2/2020 12:32	12/2/2020 12:42
7	218	22/2/2020 16:27	25/2/2020 16:36
8	224	6/3/2020 16:26	9/3/2020 16:36
9	218	19/3/2020 16:26	22/3/2020 16:35
10	214	1/4/2020 16:25	4/4/2020 16:35
11	220	14/4/2020 16:25	17/4/2020 16:34
12	220	27/4/2020 16:24	30/4/2020 16:33
13	206	10/5/2020 16:23	13/5/2020 16:32
14	197	24/5/2020 16:23	27/5/2020 16:32
15	182	6/6/2020 16:27	9/6/2020 16:36
16	N.A.*	19/6/2020 16:26	22/6/2020 16:36
17	N.A.*	2/7/2020 16:26	5/7/2020 16:46
18	N.A.*	15/7/2020 16:37	18/7/2020 16:46
19	N.A.*	28/7/2020 16:36	31/7/2020 16:46
20	172	10/8/2020 16:35	13/8/2020 16:45
21	154	23/8/2020 16:34	26/8/2020 16:44
22	N.A.*	6/9/2020 16:34	9/9/2020 16:43
23	86	19/9/2020 16:33	22/9/2020 16:43
24	88	2/10/2020 16:32	5/10/2020 16:42
25	87	15/10/2020 16:34	18/10/2020 16:44

S.I. 10: Overlay of the chromatograms of 3 blanks and sample 14 (24/5/2020 to 27/5/2020, 197 L) for two halogenated compounds. The main contributor to the background level found in the blanks is the diffusion of compounds through the Safelok system.

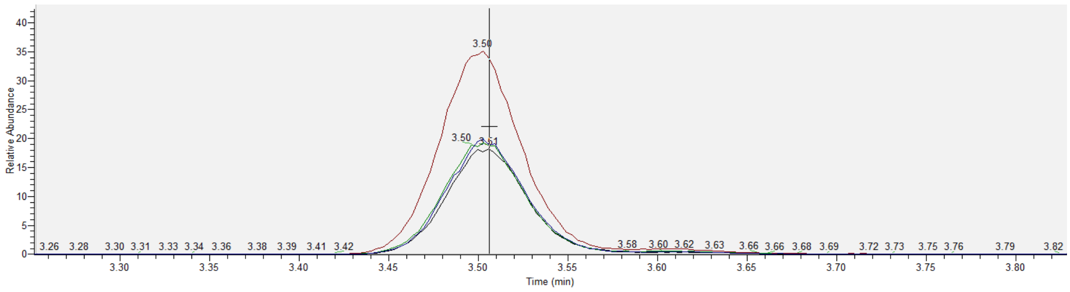

Trichloromonofluoromethane (ions: 101;103;105)

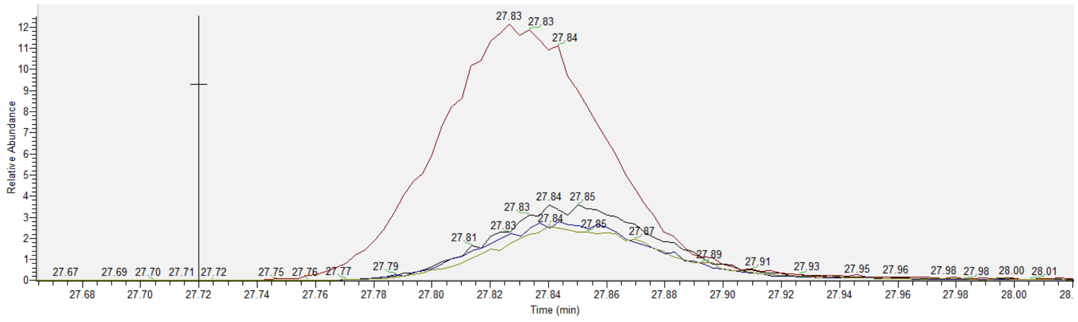

Bromoform (ions: 171;173;175)

S.I. 11: A typical time trace of a TD-PTR-Qi-TOFMS thermal desorption cycle. In this case the signal for mass 73.0284 (C3H4O2)H$^+$ methylglyoxal as recorded for sample 1 is shown.

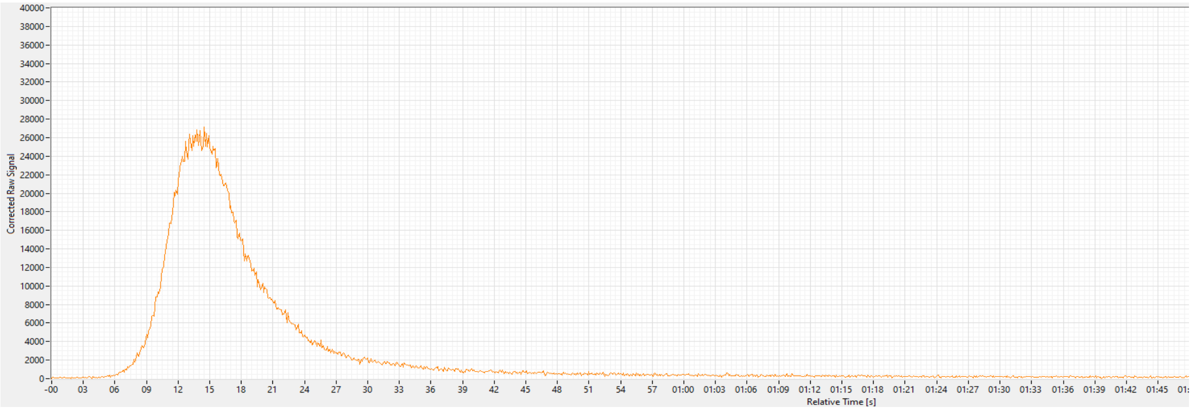

S.I. 12: The high resolution TOF-MS spectrum (red) acquired from the analysis of a sample containing methanesulfonyl chloride (CH_3ClO_2S – m(MH^+) = 114.9615). The green line represents the simulated mass spectrum of MsCl. The peak at 116.97 is a good identifier for the compound as it is caused by the abundance of the ^{37}Cl isotope.